Tests of Lepton Flavour Universality at LHCb

First Angular Analysis of $B^0 \to K^{*0} e^+ e^-$ decay at the central q^2

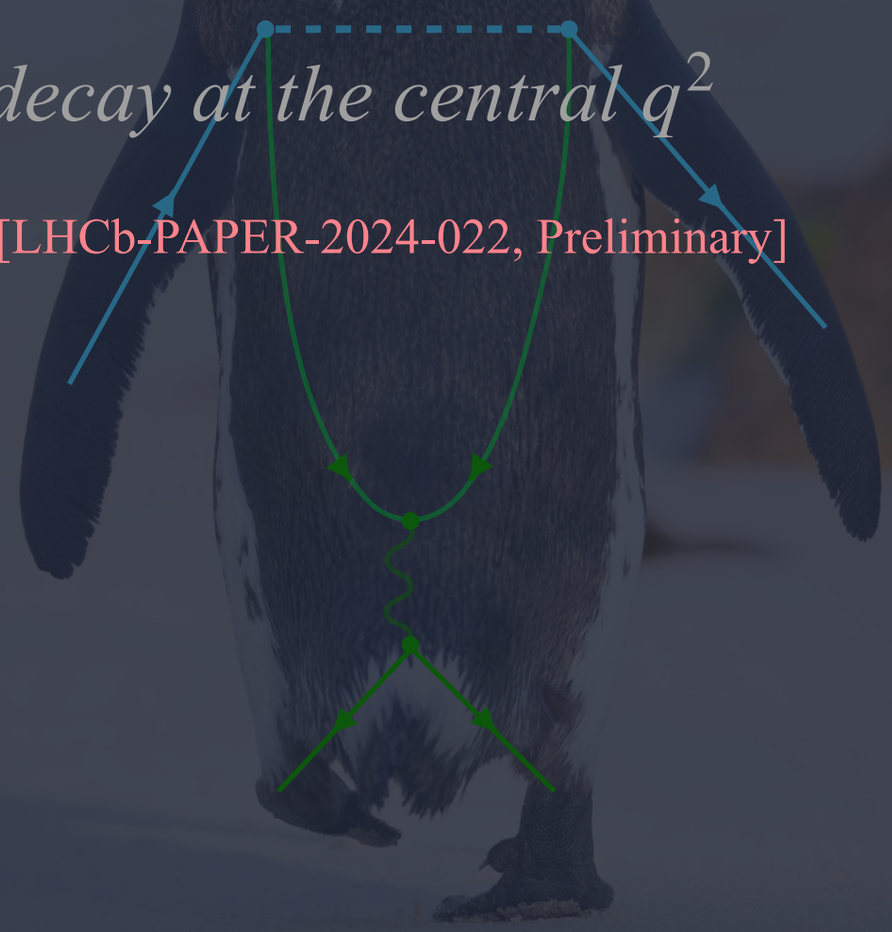

[LHCb-PAPER-2024-022, Preliminary]

Rafael Silva Coutinho

Syracuse University

On behalf of the LHCb Collaboration

42nd International Conference on High Energy Physics
Prague, July 19th, 2024

Rare Decays as a Probe of New Physics

FCNC: Unique Glimpse to Higher Scale

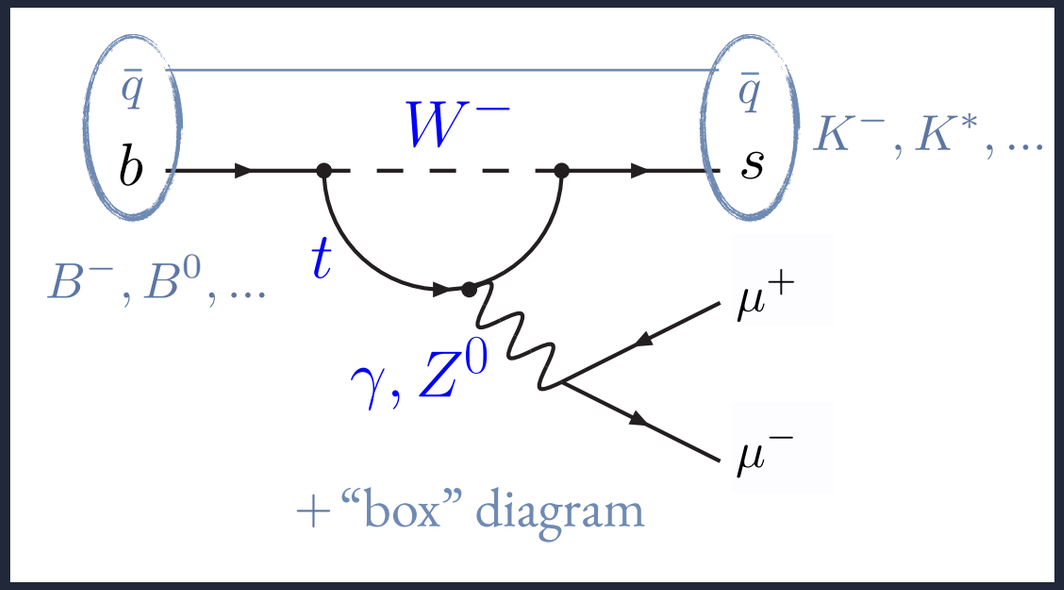

[*E.G.* enhancement/suppression of decay rate, angular distributions and new sources of ~~CP~~]

New Particles Can Contribute at Loop and/or Tree Level

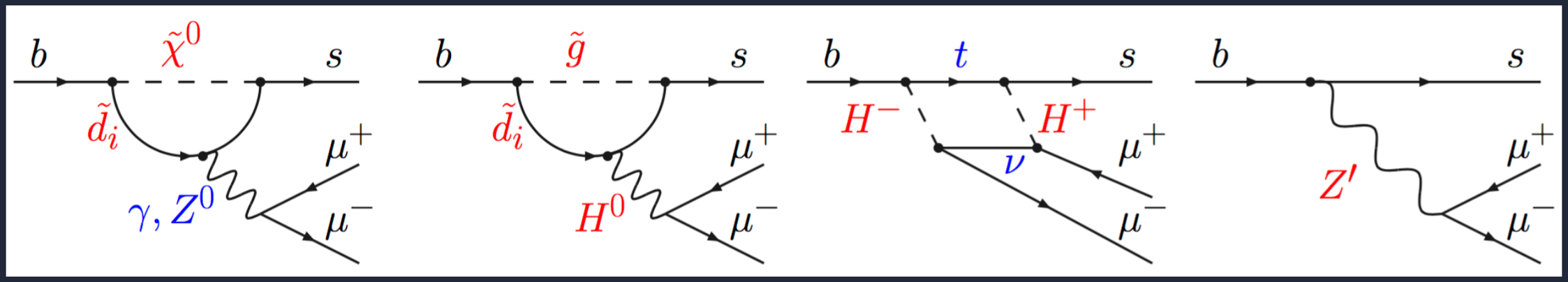

The $B^0 \to K^{*0}\ell^+\ell^-$ Decay

FCNC effective hamiltonian described as OPE

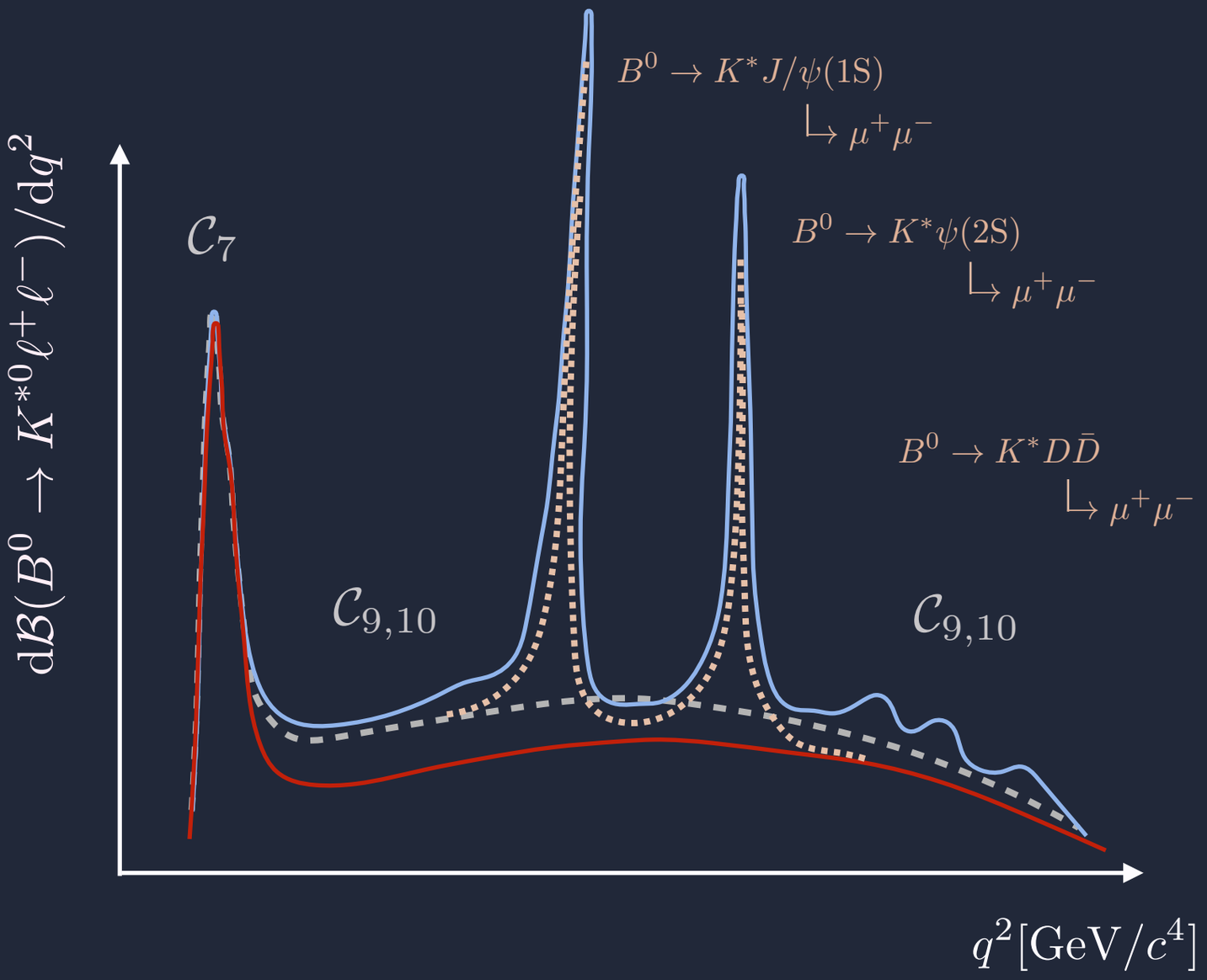

Flavour channel neutral current described in an effective field theory

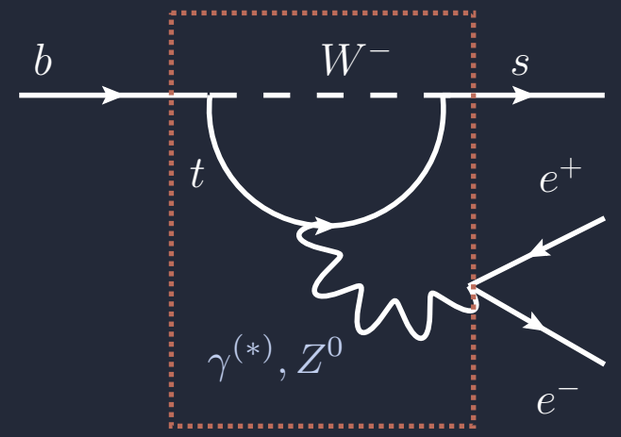

$\mathcal{C}_7, \mathcal{C}_{9,10}$

$$\mathcal{C}_i = \mathcal{C}_i^{\mathrm{SM}} + C_i^{\mathrm{NP}} + \mathcal{C}_i^{\mathrm{had}}$$

Flavour Anomalies in $b \to s\ell^+\ell^-$

<u>High</u> theoretical uncertainty

<u>Low</u> theoretical uncertainty

[Decay rate]

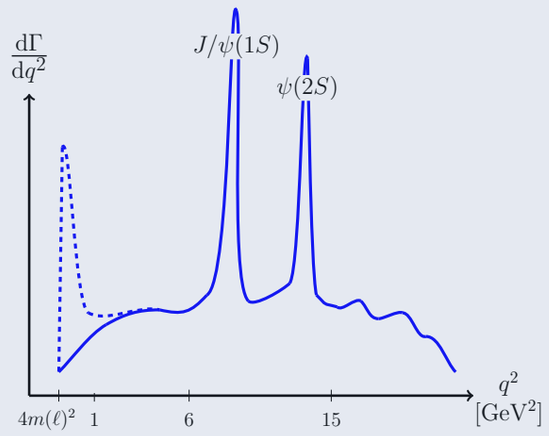

[Angular distributions]

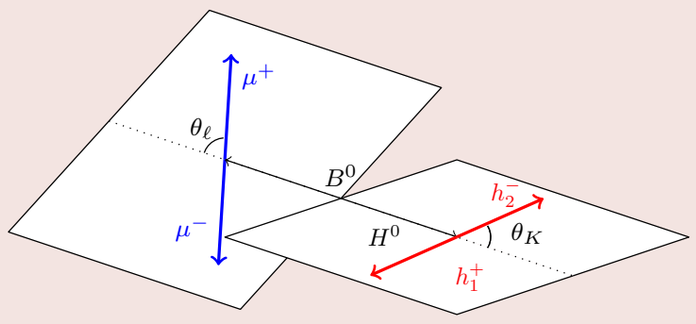

[LFU: ratio of BFs]

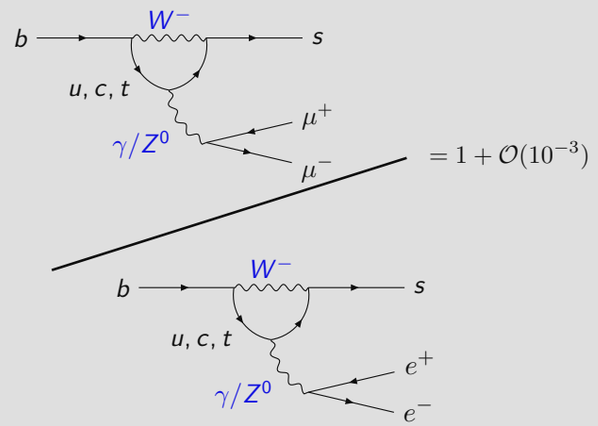

Consistent anomalous pattern

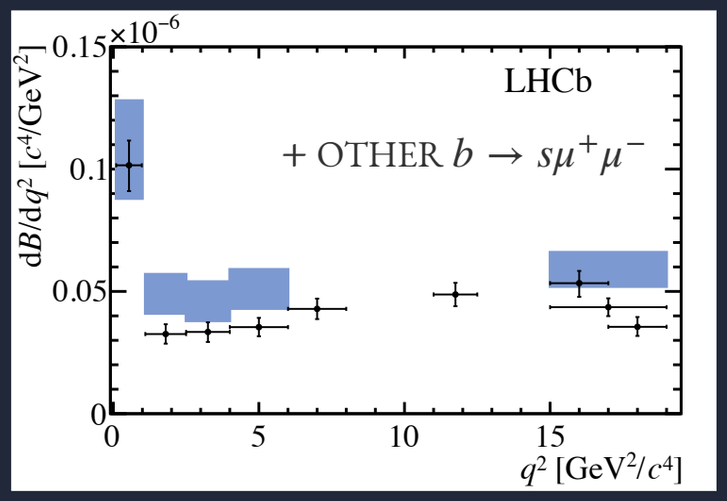

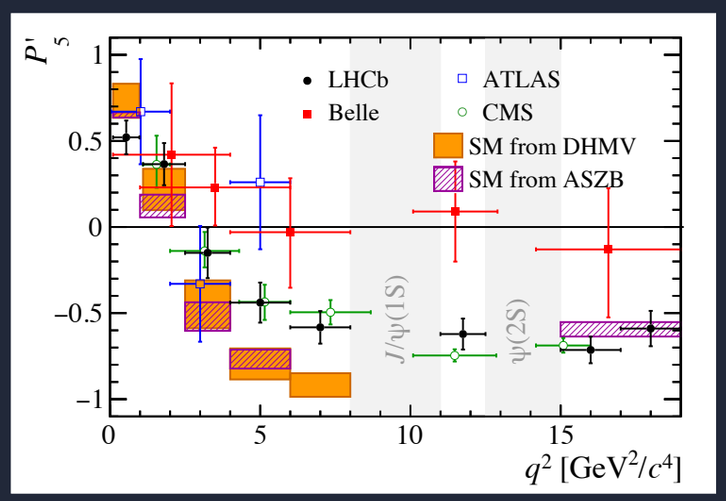

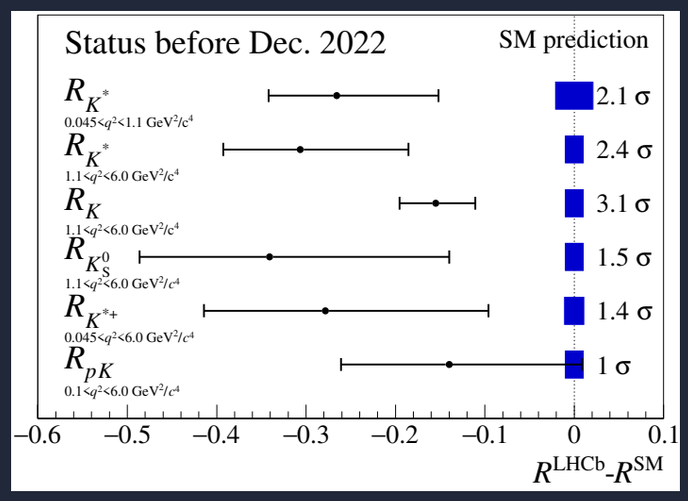

Flavour Anomalies in $b \to s\ell^+\ell^-$

High theoretical uncertainty

Low theoretical uncertainty

[Decay rate]

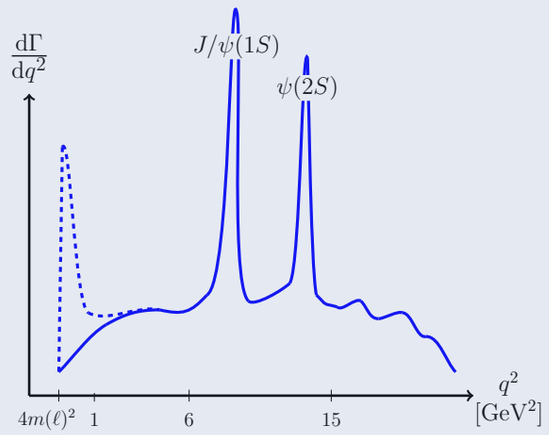

[Angular distributions]

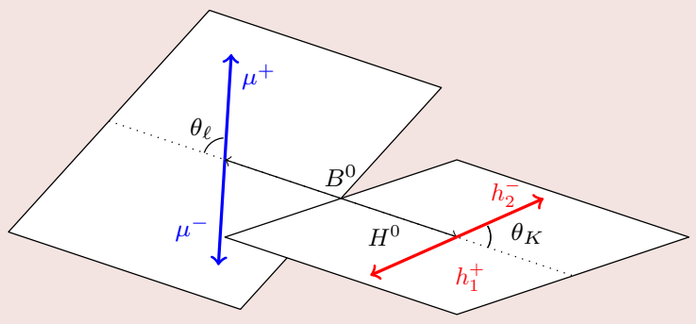

[LFU: ratio of BFs]

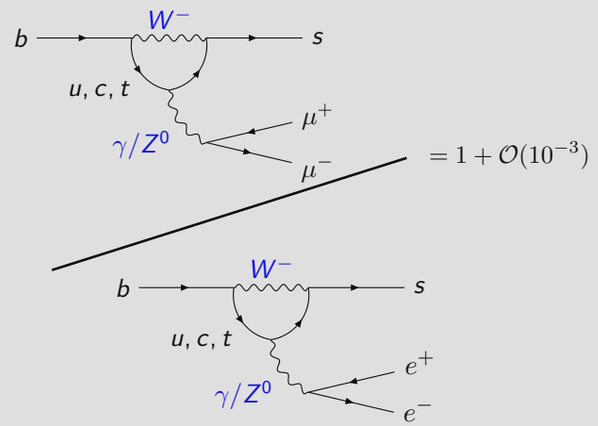

Consistent anomalous pattern

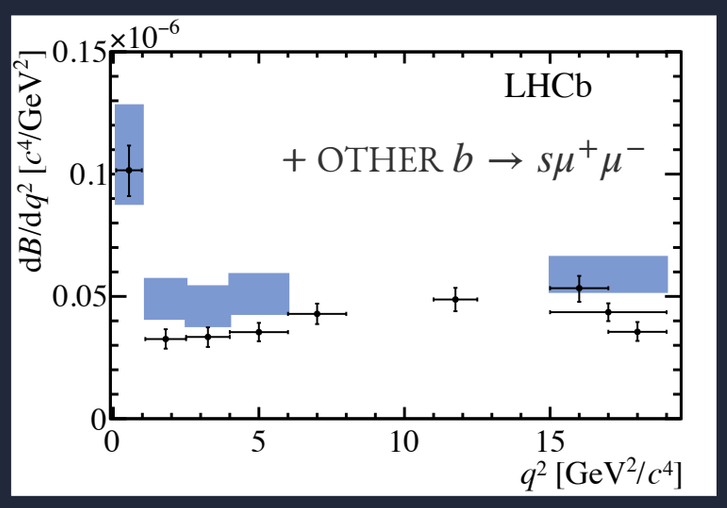

[LHCb, JHEP 11 (2016) 047]

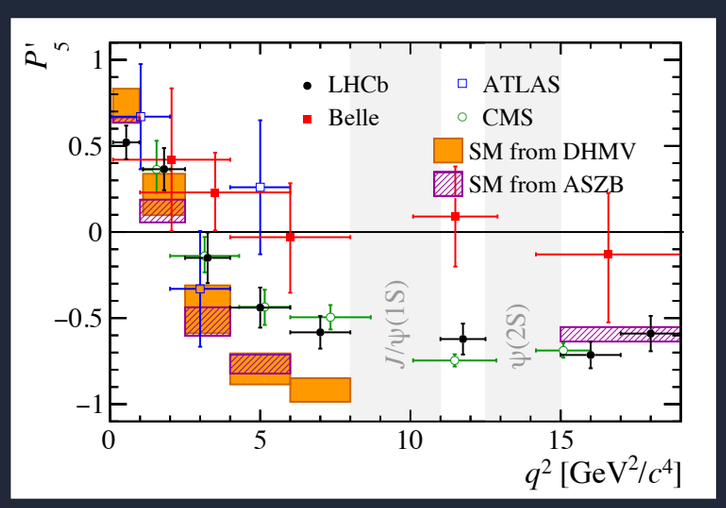

[LHCb, PRL 125 (2020) 011802
Belle, PRL 118 (2017) 11, 111801
ATLAS, JHEP 10 (2018) 047
CMS, PLB 781 (2018) 517]

LFU consistent with SM!

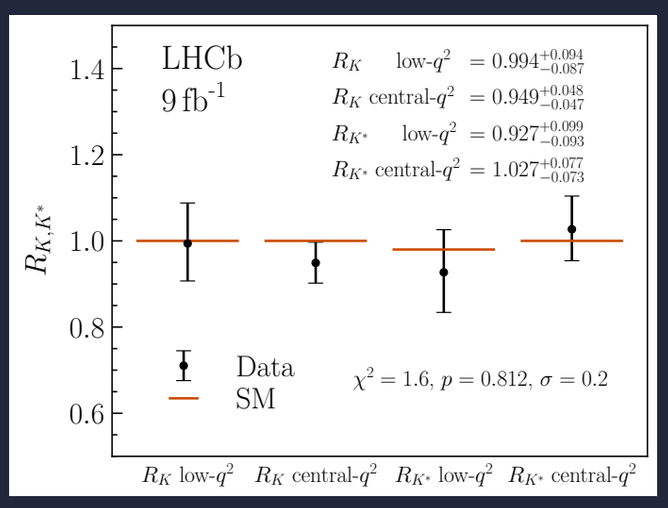

[LHCb,PRL 131 (2023) 051803, PRD 108 (2023) 032002]

Flavour Anomalies in $b \to s\ell^+\ell^-$

High theoretical uncertainty

Low theoretical uncertainty

[Decay rate]

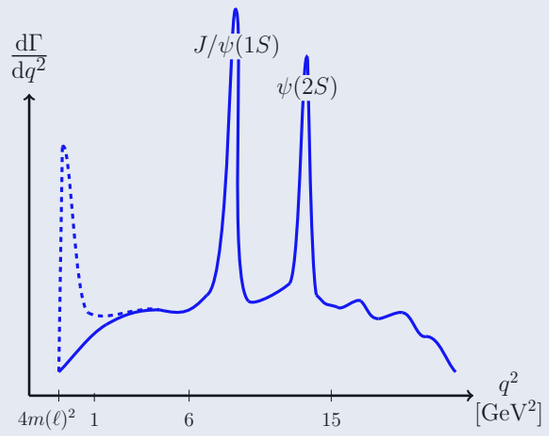

[Angular distributions]

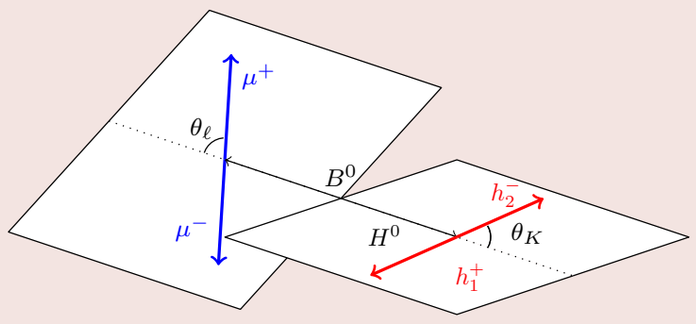

[LFU: ratio of BFs]

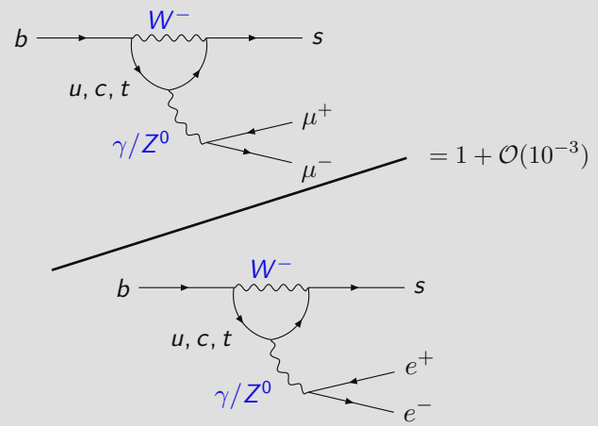

What about LFU tests in angular distributions?

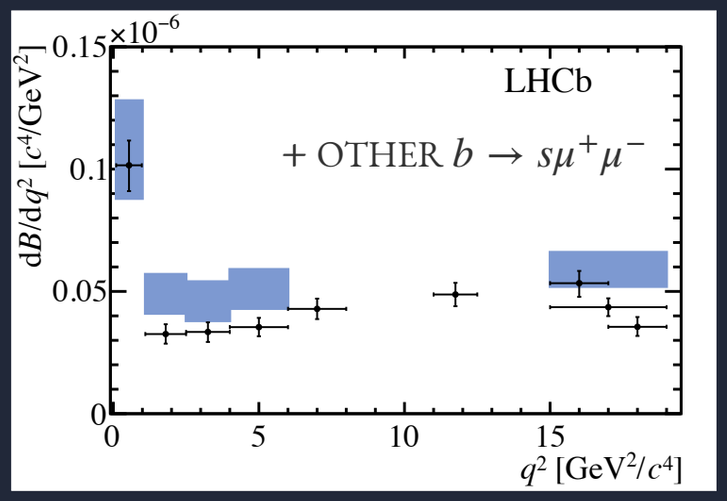

[LHCb, JHEP 11 (2016) 047]

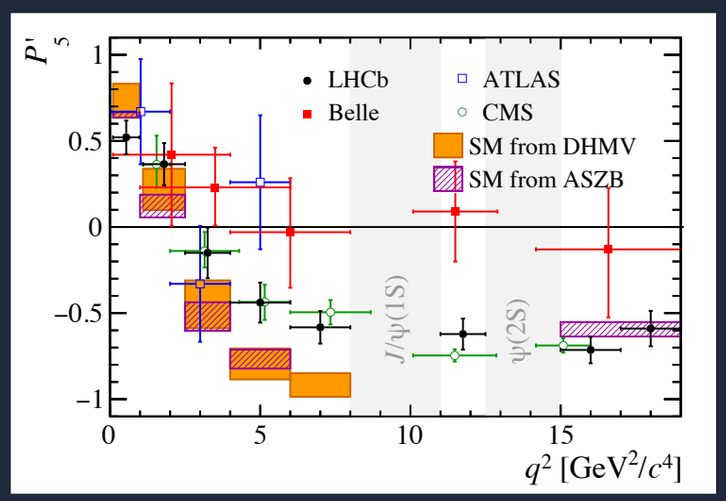

[LHCb, PRL 125 (2020) 011802
Belle, PRL 118 (2017) 11, 111801
ATLAS, JHEP 10 (2018) 047
CMS, PLB 781 (2018) 517]

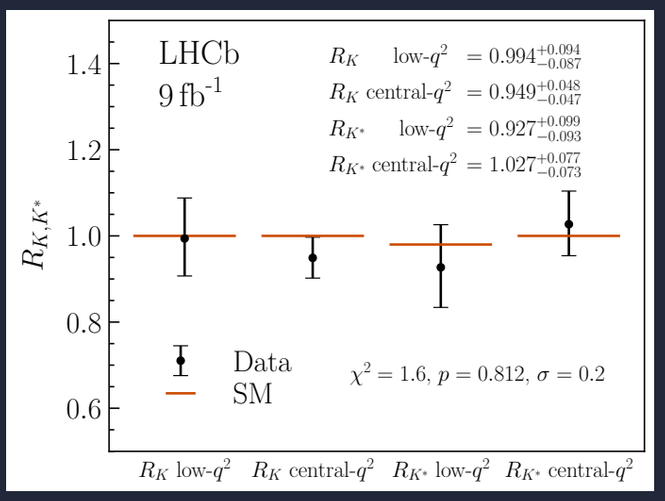

[LHCb,PRL 131 (2023) 051803, PRD 108 (2023) 032002]

Analysis Strategy

[LHCb-PAPER-2024-022, Preliminary]

First angular analysis of $B^0 \to K^{*0} e^+ e^-$ decays at the central q^2 region

- Full Run 1 + 2 LHCb statistics ($9\,\text{fb}^{-1}$)
  - Simultaneous fit to [2011-2012], [2015-2016] and [2017-2018] datasets
- 4D unbinned weighted fit to the mass and angular distributions

$$\text{PDF}(\vec{\Omega}, m|\vec{\Theta}, \vec{\lambda}) = f_{sig}\text{pdf}_{sig}(\vec{\Omega}, m||\vec{\Theta}, \vec{\lambda}) + \sum_i^{n-1} f_{bkg,i}\text{pdf}_{bkg,i}(\vec{\Omega}, m|\vec{\lambda}_{bkg,i}) + (1 - f_{sig} - \sum_i^{n-1} f_{bkg,i})\text{pdf}_{bkg,n}(\vec{\Omega}, m|\vec{\lambda}_{bkg,n})$$

With likelihood as $$-\sum_{events,e} \frac{1}{\epsilon_e(\vec{\Omega}, q^2)} \cdot \ln \text{PDF}(\vec{\Omega}, m|\vec{\Theta}, \vec{\lambda})$$

Mass an angular distributions are assumed to factorise

- Selection and corrections follow closely R_{K*} analysis
  [PRL 131 (2023) 051803, PRD 108 (2023) 032002]
- Determine CP-averaged S_i and corresponding optimised $P_i^{(\prime)}$ observables
- LFU observables Q_i are derived by comparing the results against previously published LHCb muon analysis

$$Q_i = P_i^{(\mu)} - P_i^{(e)}$$

[JHEP 10 (2016) 075]

The rare decay $B^0 \to K^{*0}[K^+\pi^-]e^+e^-$

Decay fully described by three helicity angles

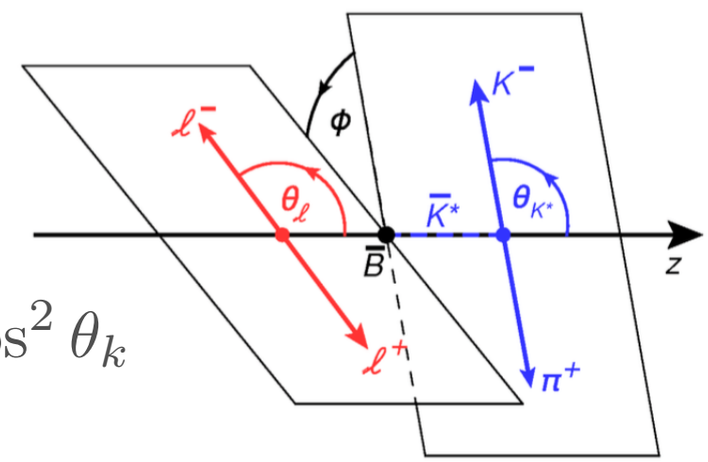

$$\frac{1}{d(\Gamma+\bar{\Gamma})/dq^2}\frac{d^4(\Gamma+\bar{\Gamma})}{dq^2\,d\vec{\Omega}} = \frac{9}{32\pi}\Big[\tfrac{3}{4}(1-F_{\rm L})\sin^2\theta_k + F_{\rm L}\cos^2\theta_k$$
$$+\tfrac{1}{4}(1-F_{\rm L})\sin^2\theta_k\cos 2\theta_l$$
$$-F_{\rm L}\cos^2\theta_k\cos 2\theta_l + S_3\sin^2\theta_k\sin^2\theta_l\cos 2\phi$$
$$+S_4\sin 2\theta_k\sin 2\theta_l\cos\phi + S_5\sin 2\theta_k\sin\theta_l\cos\phi$$
$$+\tfrac{4}{3}A_{\rm FB}\sin^2\theta_k\cos\theta_l + S_7\sin 2\theta_k\sin\theta_l\sin\phi$$
$$+S_8\sin 2\theta_k\sin 2\theta_l\sin\phi + S_9\sin^2\theta_k\sin^2\theta_l\sin 2\phi\Big]$$

Fraction of longitudinal polarisation of the K*

Forward-backward asymmetry of the di-lepton system

F_L, A_{FB} and S_i are combinations of K^{*0} spin amplitudes sensitive to $C^{(\prime)}_{7,9,10}$ and form factors

Perform ratios of observables (e.g. P_5') where form factors cancel at leading order

$$P_5' = \frac{S_5}{\sqrt{F_{\rm L}(1-F_{\rm L})}}$$ [JHEP 1204 (2012) 104]

*S-wave contribution is considered in the systematics

Data Selection

Improved strategy to control signal resolution in electrons:

q^2 defined with B^0 primary vertex and B^0 mass constraint, allowing for the extension of the analysis range up to 7.0 GeV^2/c^4 and reduced bin migration

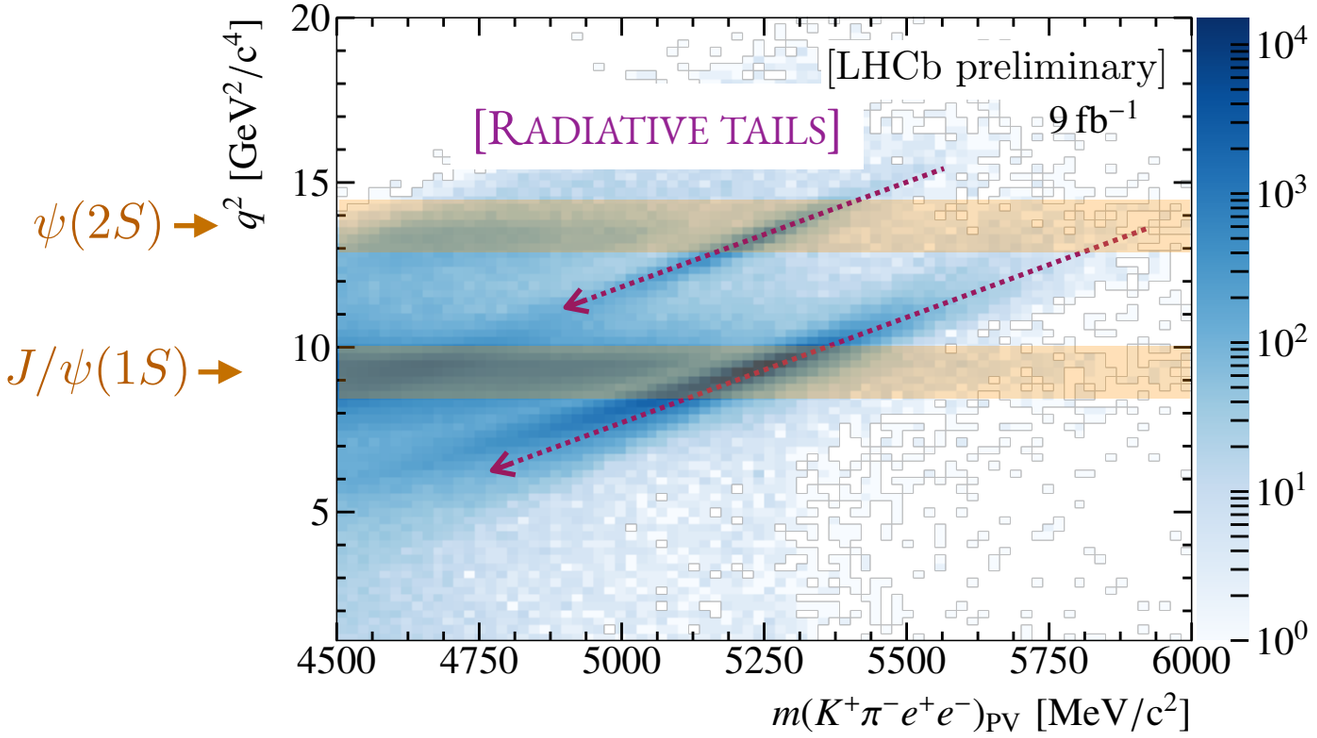

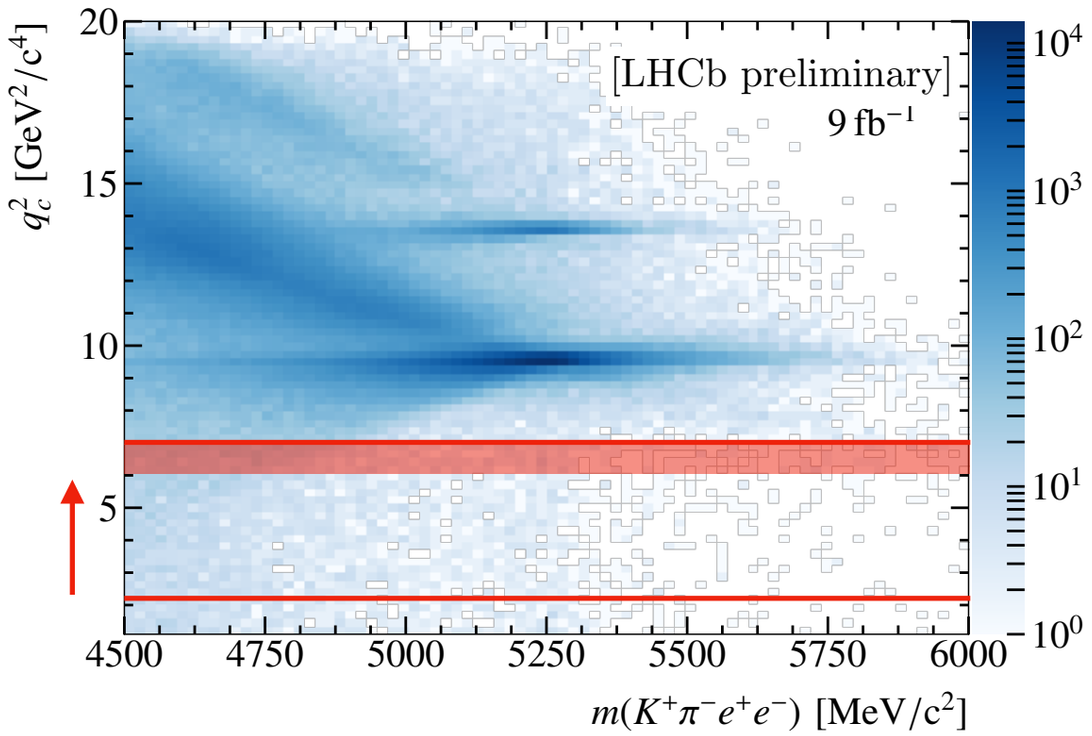

Analysis performed in two q^2 regimes: [1.1, 6.0] and [1.1, 7.0] GeV^2/c^4

Acceptance Effects

Angular and q^2 distributions are distorted by the efficiency of the selection and reconstruction, and resolution effects

Efficiency parametrised in 4D using Legendre polynomial for all variables except phi (Fourier):

$$\epsilon(\cos\theta_\ell, \cos\theta_K, \phi, q_c^2) = \sum_{k,l,m,n} c_{k,l,m,n} L_k(\cos\theta_K) L_l(\cos\theta_\ell) F_m(\phi) L_n(q_c^2)$$

Coefficients are obtained from simulation using method of moments:

$$c_{k,l,m,n} = \frac{1}{N'} \sum_{i=1}^{N} w_i \left[\left(\frac{2k+1}{2}\right) \left(\frac{2l+1}{2}\right) \left(\frac{2m+1}{2}\right) \left(\frac{2n+1}{2}\right) \right]$$

Weights account for data simulation differences

Signal/background Separation

Control over background contributions requires knowledge of the mass and angular structure

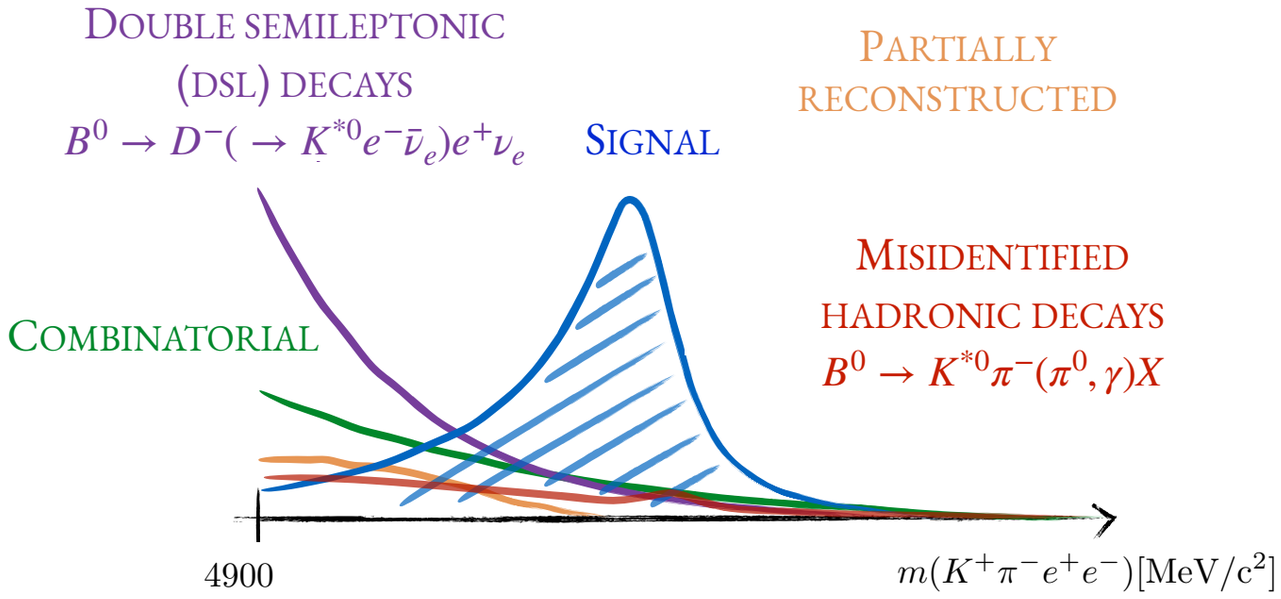

Data-driven strategy used to obtain an effective lineshape using control samples

Pass-fail method (inverted PID)

[PRL 131 (2023) 051803, PRD 108 (2023) 032002]

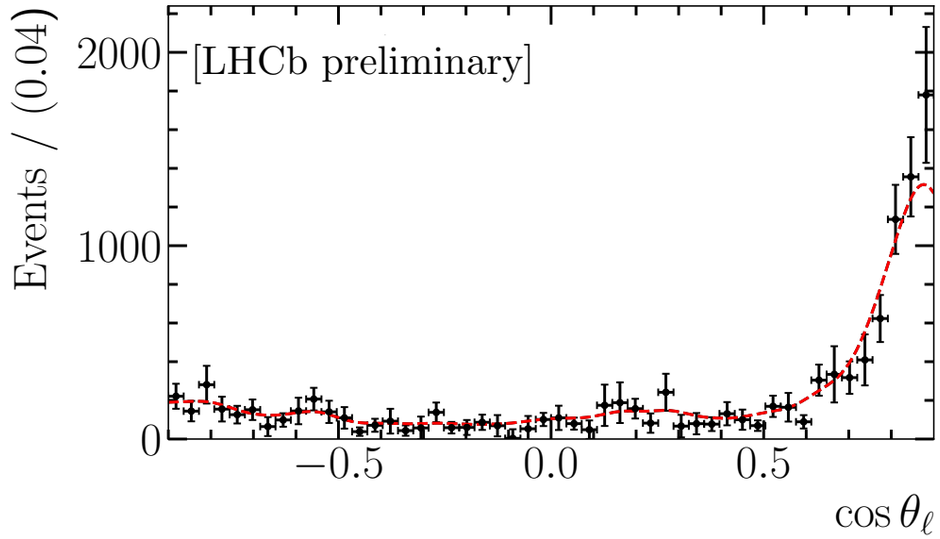

$B^0 \to K^{*0}e^+\mu^-$(LFV) data

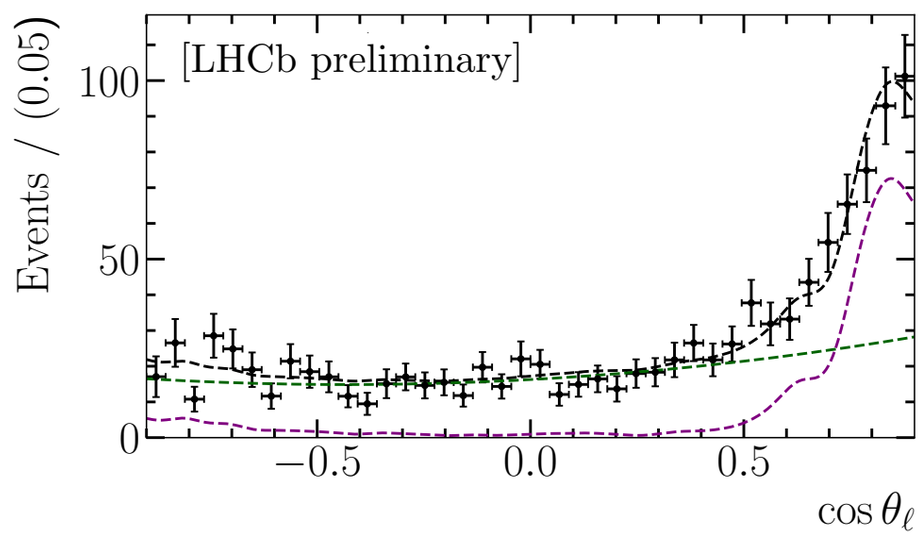

Systematic Uncertainties

Largest uncertainties are mostly associated to assumptions on the effective background modelling

	F_L	S_3	S_4	S_5	A_{FB}	S_7	S_8	S_9
DSL and comb.	0.687	0.372	0.297	0.321	0.449	0.177	0.668	0.294
Part. reco.	0.091	0.039	0.039	0.049	0.051	0.021	0.034	0.037
Had. misid.	0.376	0.254	0.107	0.178	0.155	0.336	0.129	0.141
Effective acceptance	0.399	0.249	0.419	0.410	0.331	0.508	0.393	0.214
Signal mass modelling	0.254	0.057	0.071	0.111	0.122	0.044	0.045	0.062
Residual backgrounds	0.179	0.039	0.045	0.062	0.137	0.032	0.032	0.047
S-wave component	0.351	0.050	0.129	0.084	0.105	0.159	0.008	0.103
B^+ veto	0.499	0.133	0.152	0.179	0.242	0.159	0.154	0.117
Fit bias	0.007	0.008	0.030	0.038	0.042	0.007	0.019	0.031
Total*	1.118	0.540	0.570	0.601	0.665	0.676	0.804	0.430

*Values are given relative to the statistical uncertainties

- F_L, A_{FB} and S_8 are particularly affected by choices on the double semileptonic and combinatorial parametrisation
- Sizeable impact of the acceptance modelling (data/simulation corrections)

Data Fit Projections

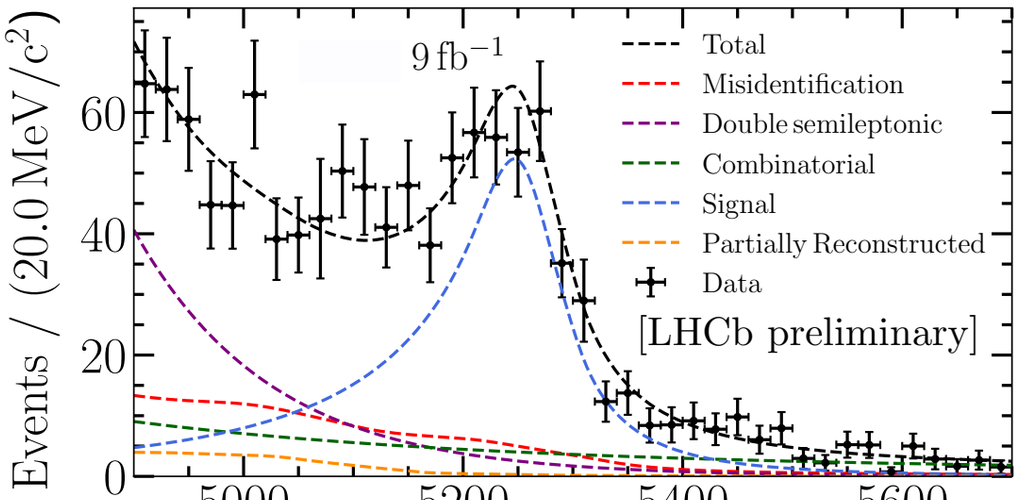

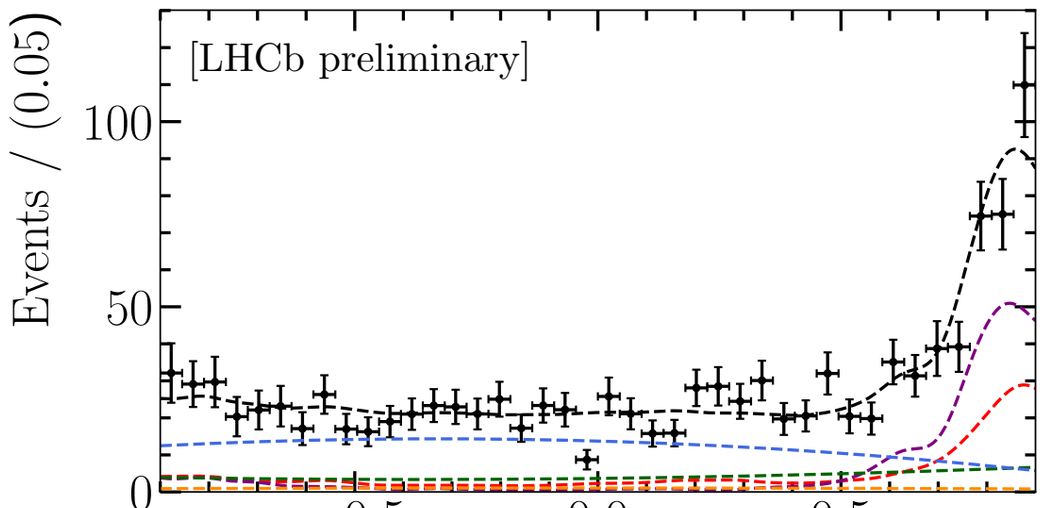

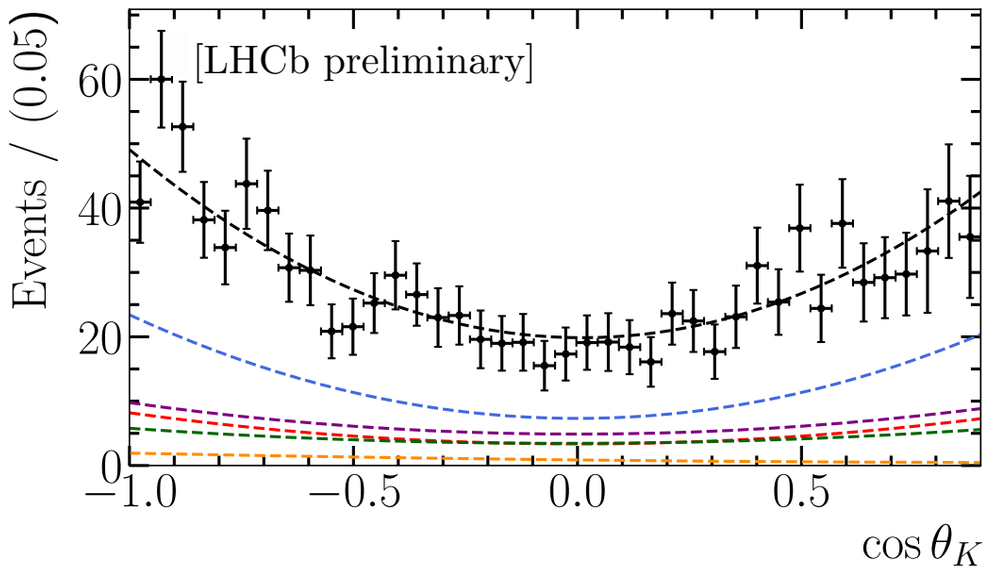

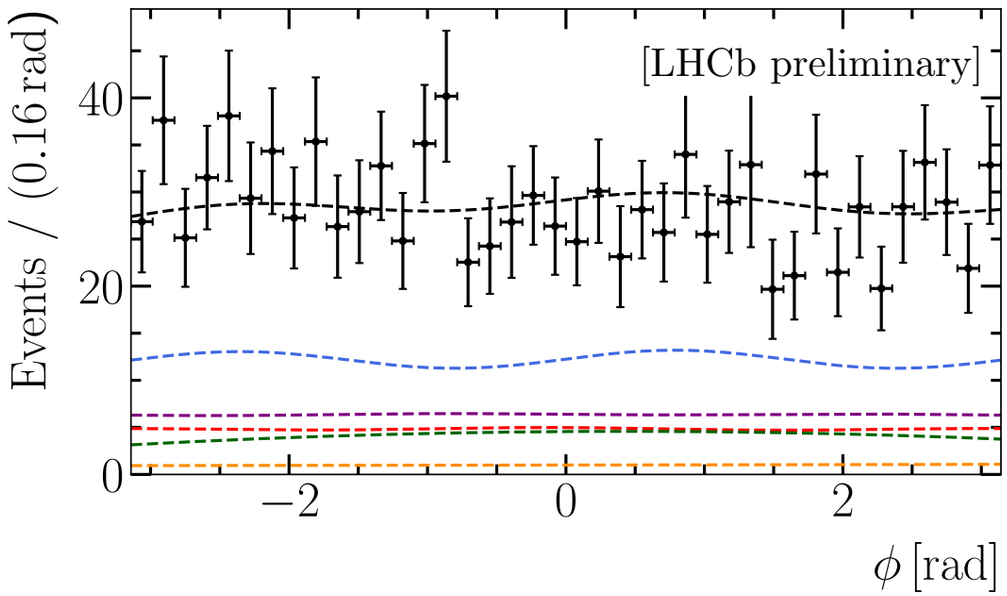

Data Fit Results Summary

$1.1 < q^2 < 6.0\,\mathrm{GeV}^2/c^4$			
F_L	$0.582 \pm 0.045 \pm 0.050$		
S_3	$-0.000 \pm 0.042 \pm 0.023$	P_1	$-0.002 \pm 0.202 \pm 0.246$
S_4	$-0.119 \pm 0.073 \pm 0.042$	P_4'	$-0.242 \pm 0.148 \pm 0.120$
S_5	$-0.077 \pm 0.054 \pm 0.033$	P_5'	$-0.157 \pm 0.110 \pm 0.102$
A_FB	$-0.146 \pm 0.052 \pm 0.035$	P_2	$-0.232 \pm 0.083 \pm 0.112$
S_7	$-0.077 \pm 0.056 \pm 0.038$	P_6'	$-0.155 \pm 0.114 \pm 0.092$
S_8	$0.129 \pm 0.072 \pm 0.056$	P_8'	$0.262 \pm 0.146 \pm 0.137$
S_9	$0.066 \pm 0.045 \pm 0.020$	P_3	$-0.157 \pm 0.107 \pm 0.110$

Overall good agreement with SM predictions

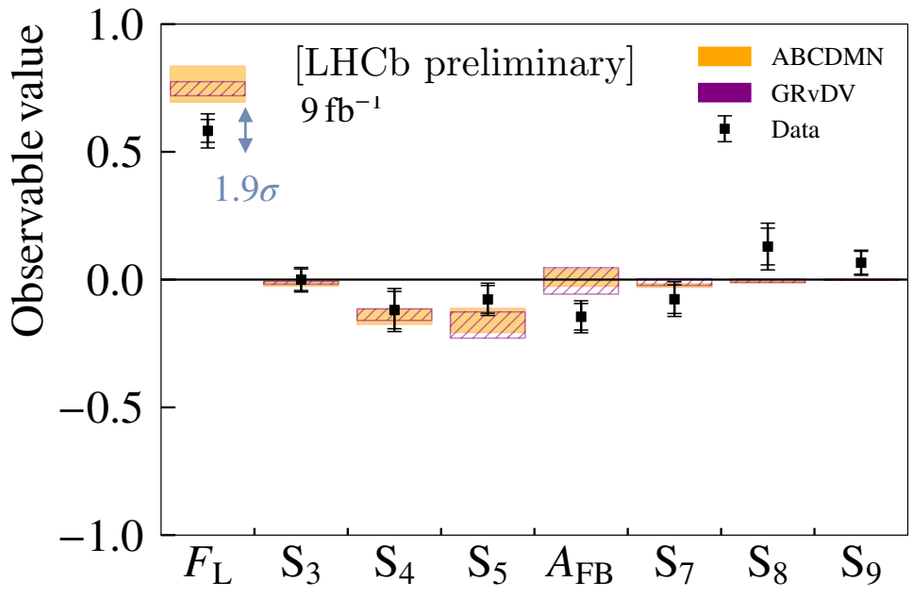

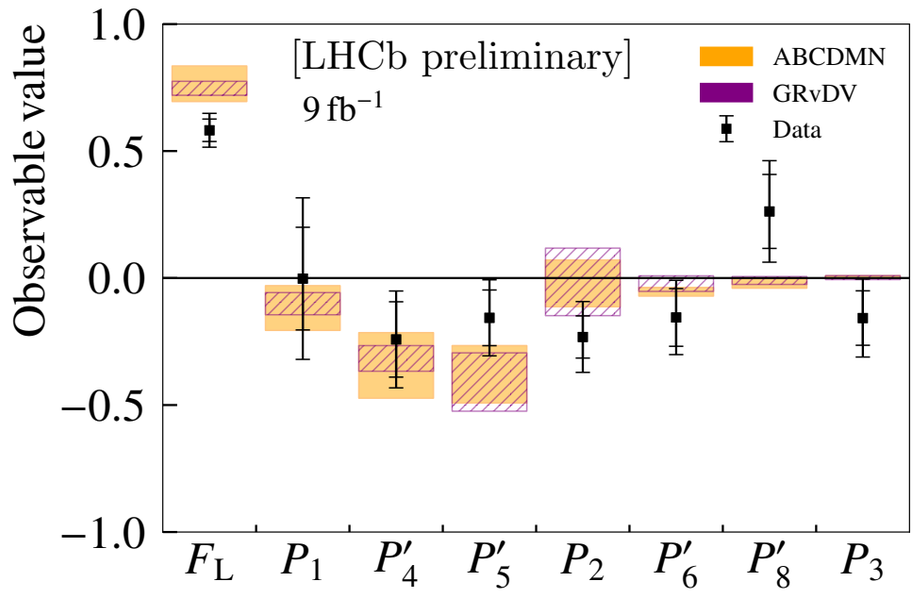

[N. Gubernari, M. Reboud, D. Van Dyk, J. Virto, JHEP 09 (2022) 133

[M. Algueró, A. Biswas, B.Capdevila, S. Descotes-Genon, J. Matias, EPJC 83 (2023) 7, 648

Optimised Angular Observables

Similar pattern observed in the $P_i^{(\prime)}$ basis

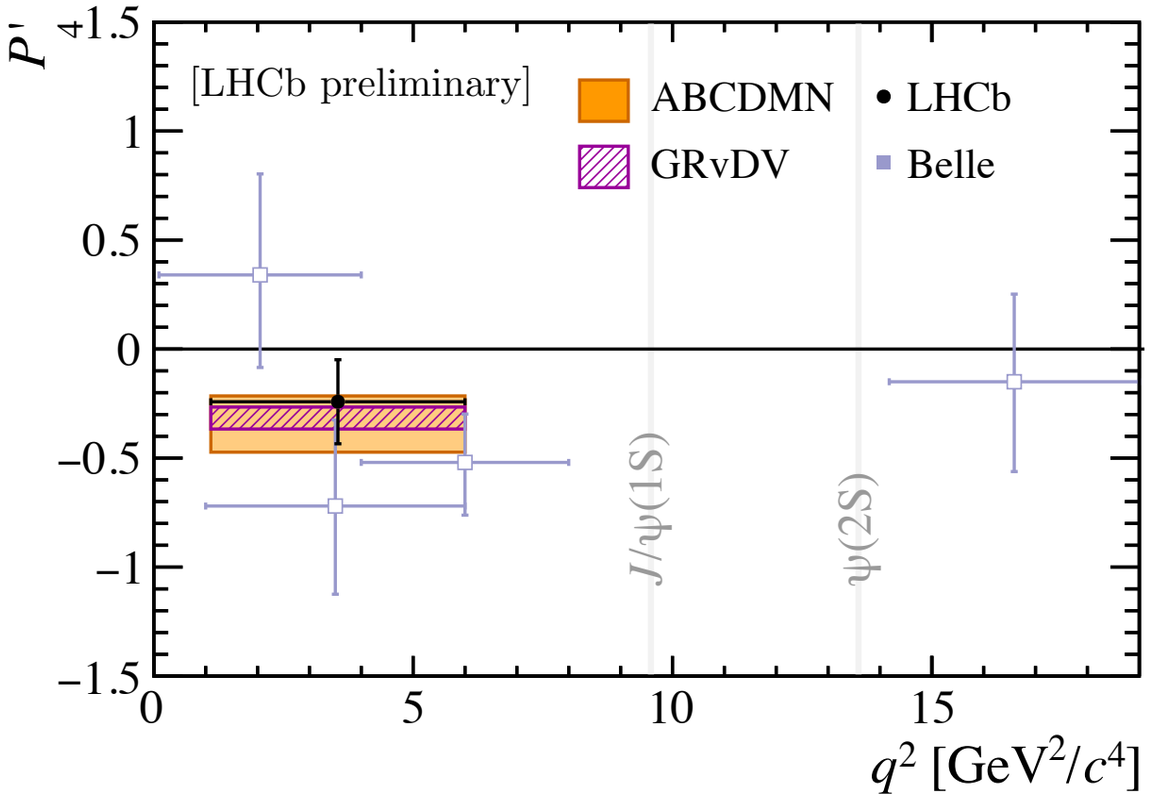

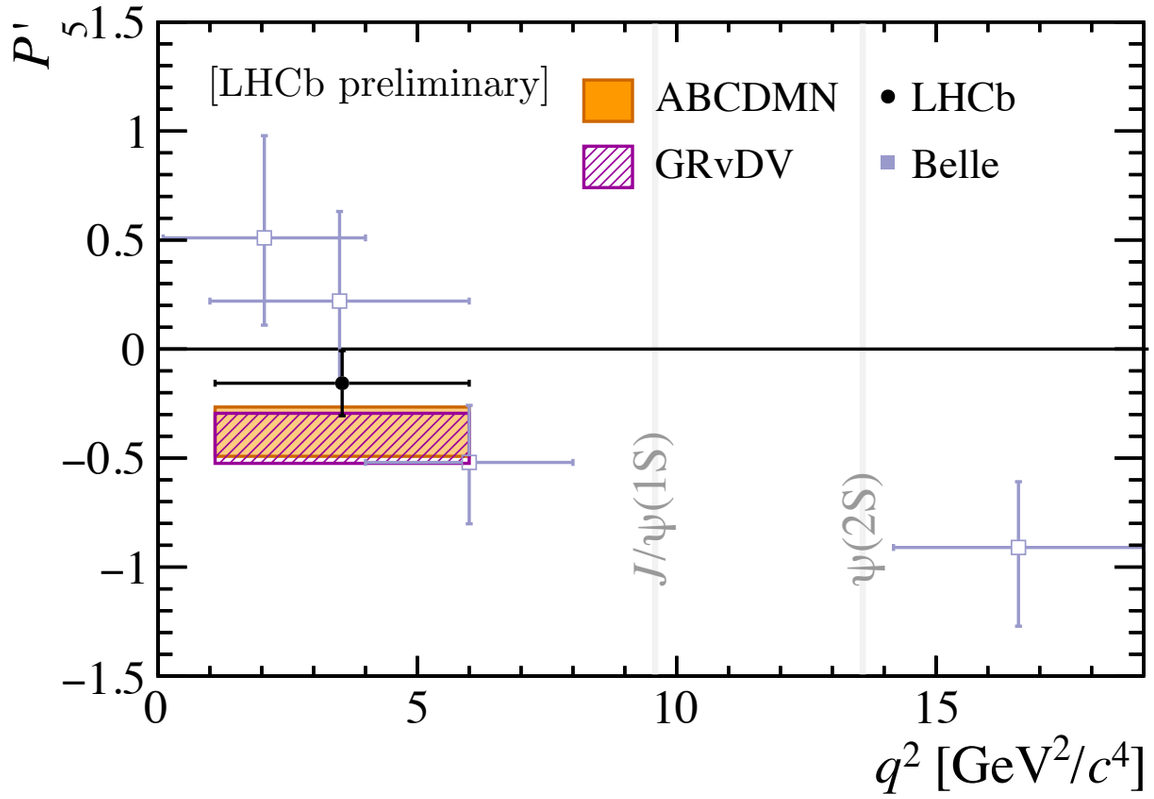

Most precise determination of angular observables

[Belle Collaboration, PRL 118 (2017) 111801

[N. Gubernari, M. Reboud, D. Van Dyk, J. Virto, JHEP 09 (2022) 133

[M. Algueró, A. Biswas, B.Capdevila, S. Descotes-Genon, J. Matias, EPJC 83 (2023) 7, 648

LFU Angular Observables

LFU quantities are derived by comparing with muon results [PRL 132 (2024) 131801]*

$$Q_i = P_i^{(\mu)} - P_i^{(e)}$$

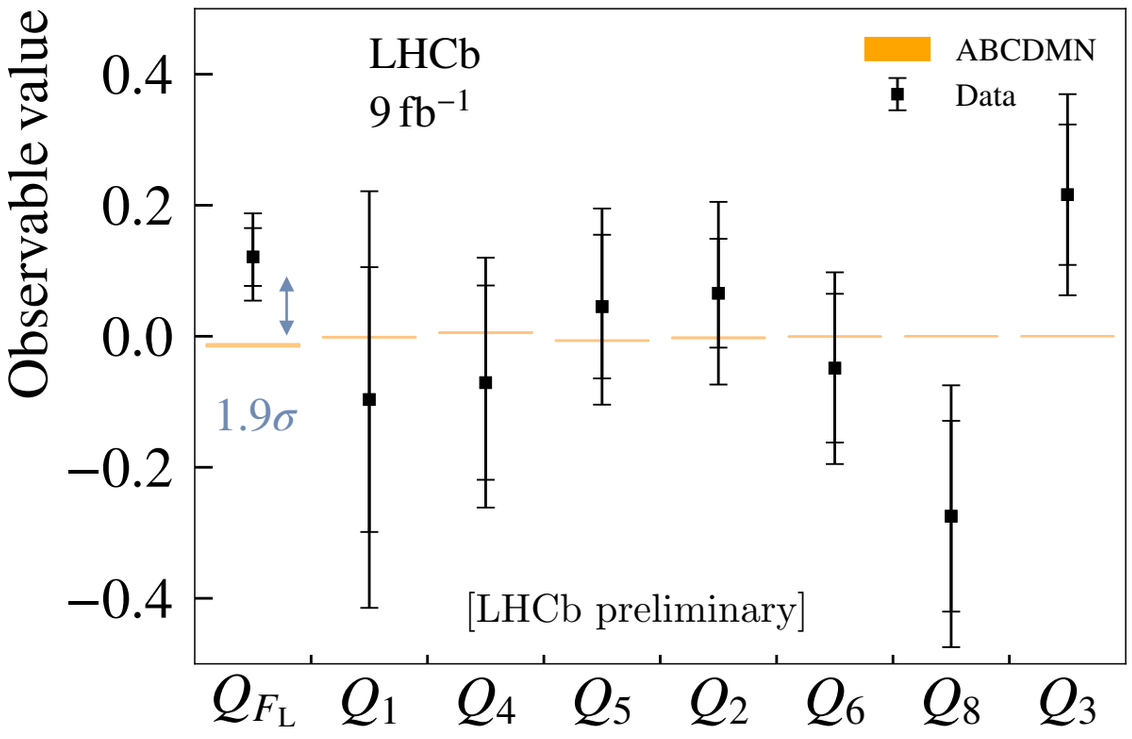

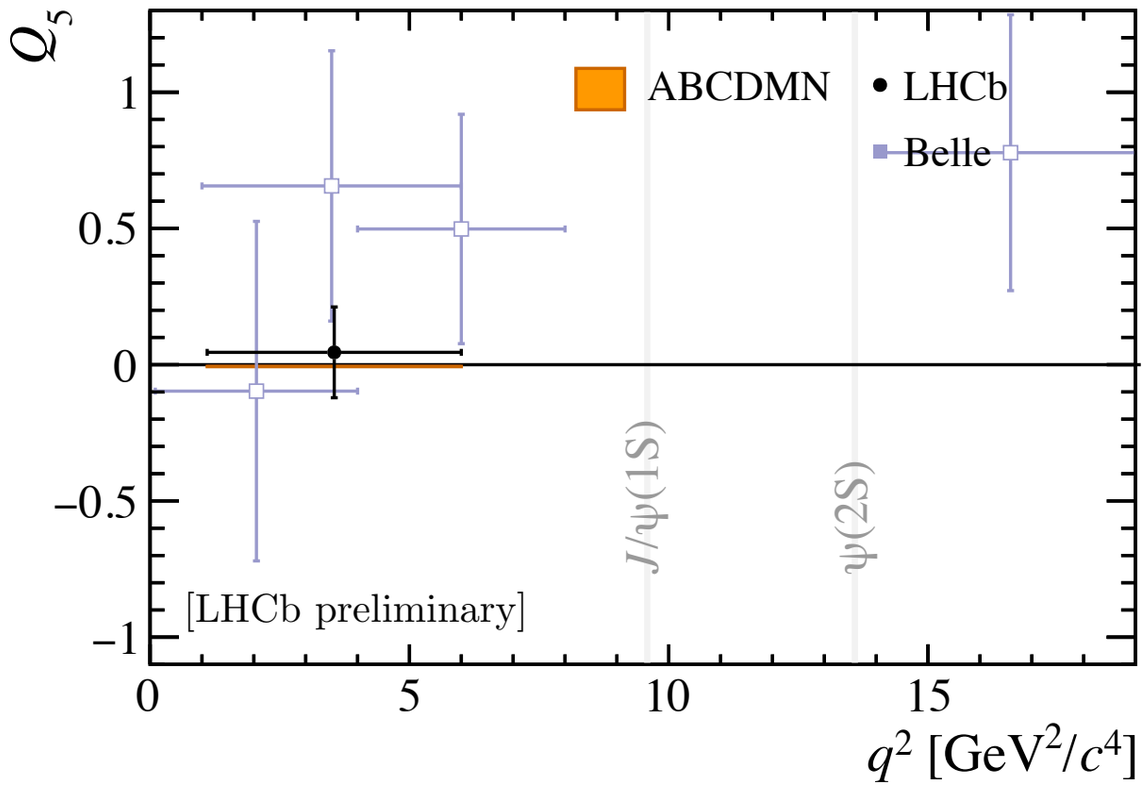

Results are all consistent with the LFU conservation hypothesis

[Belle Collaboration, PRL 118 (2017) 111801

[M. Algueró, A. Biswas, B.Capdevila, S. Descotes-Genon, J. Matias, EPJC 83 (2023) 7, 648

*Muon data re-analysed without explicit S-wave contribution

Wilson Coefficient Interpretation

A global fit with all angular observables is performed varying $Re(C_9)$:

- Form factors constrained from [JHEP 12 (2023) 153] and non-local QCD terms from [JHEP 02 (2021) 088, JHEP 09 (2022) 133]
- Local and non-local hadronic contributions are shared for the two lepton species

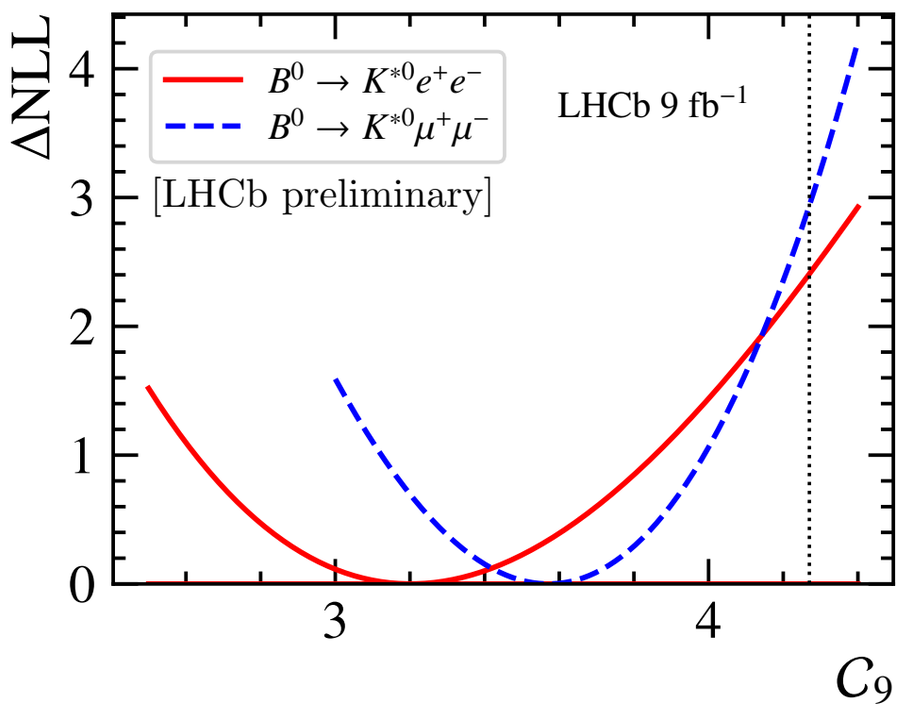

Similar pattern of shift in $Re(C_9)$

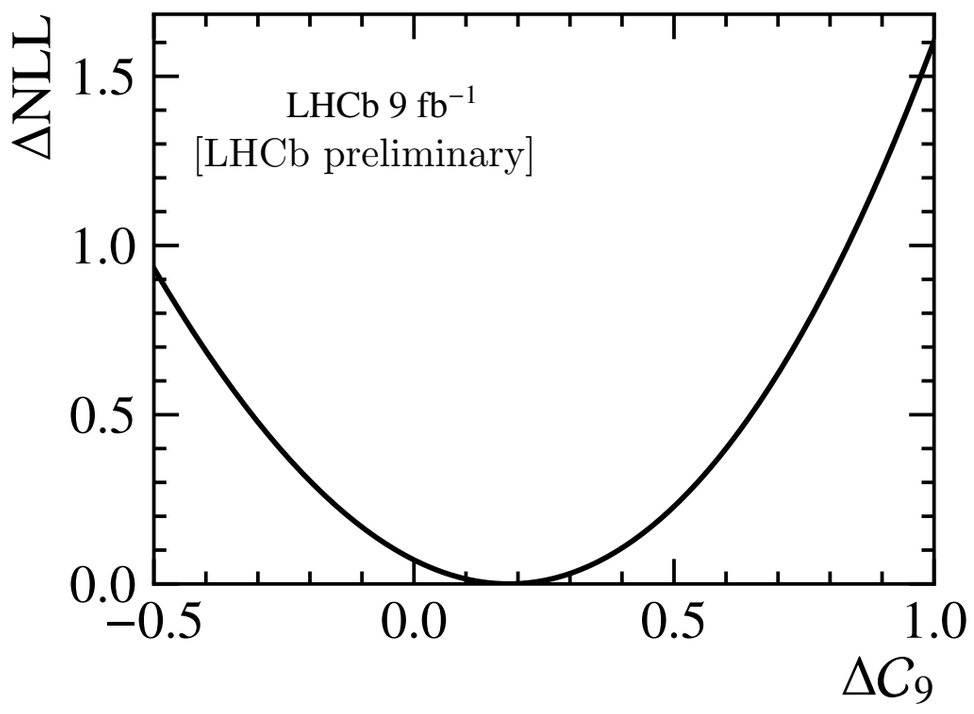

$\Delta C_9 = C_9^{(\mu)} - C_9^{(e)}$ consistent with zero

Summary

- First angular analysis for electrons in the central q^2 region at hadronic machines

- Best precision of angular observables

Sensitivity at the same level as first P_5' measurement in muons

- Results are consistent with the SM and with the LFU hypothesis

- A global fit to the angular observables favours a similar pattern of shift in $Re(C_9)$ as in the $b \to s\mu^+\mu^-$ anomalies

- Measurement opens experimental venue for high-precision LFU/angular analysis with data from Run 3 and beyond

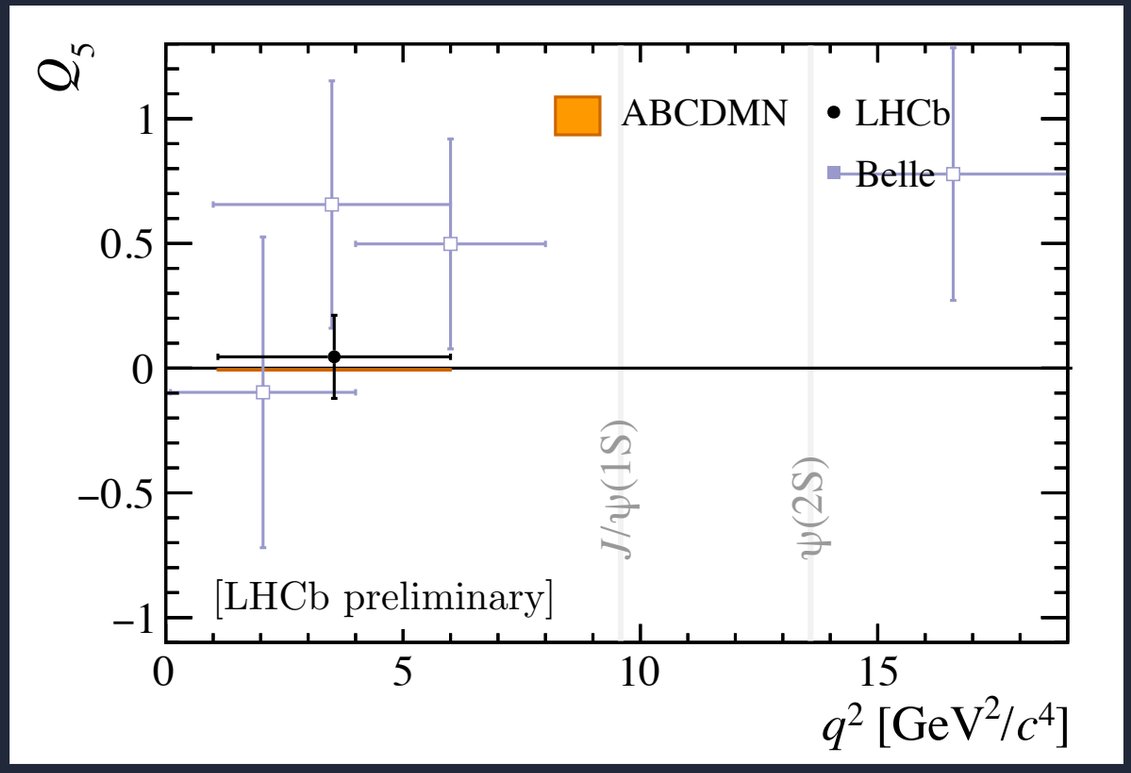

The LHCb experiment

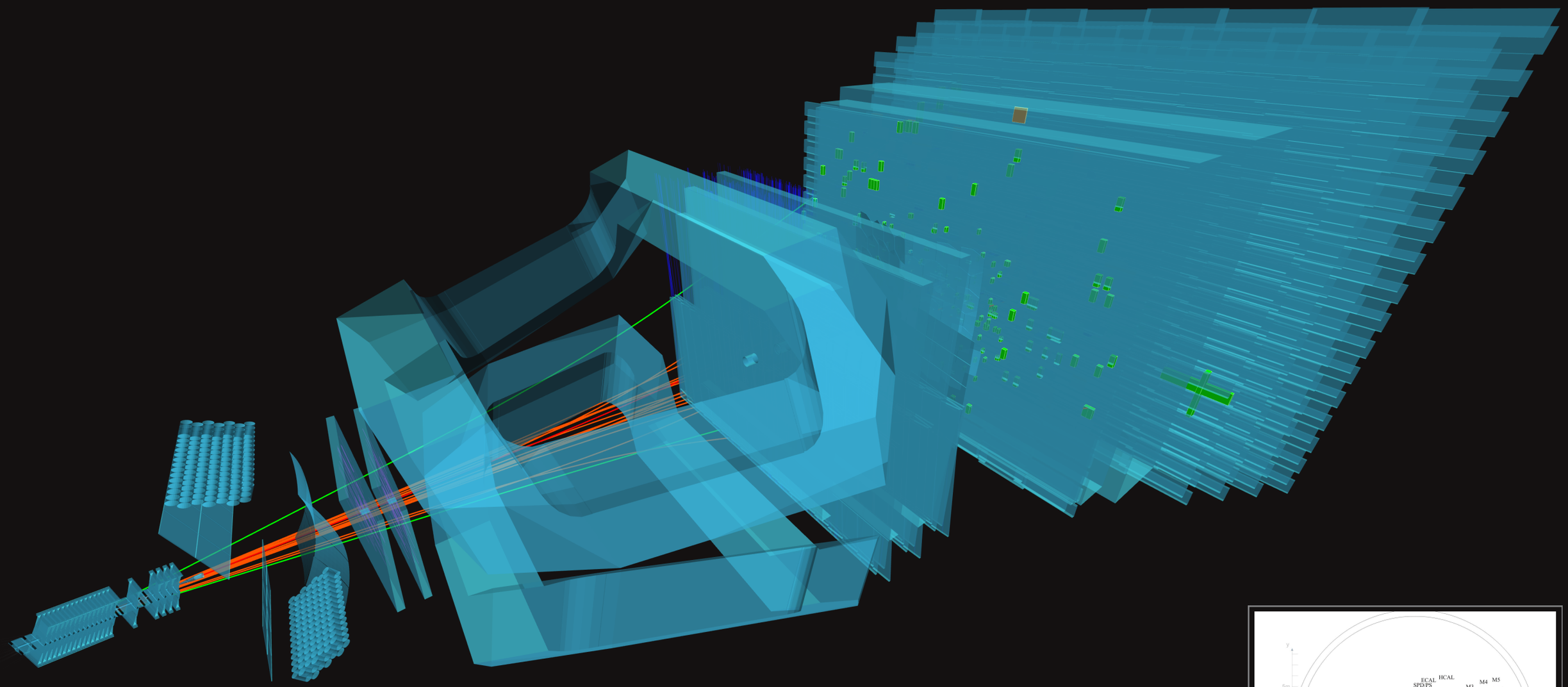

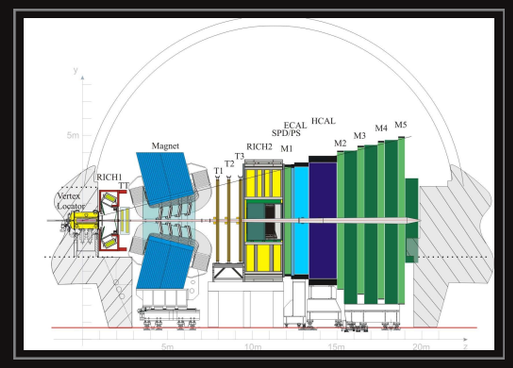

[Int. J. Mod. Phys. A30, (2015) 1530022]

[Backup]

The LHCb experiment

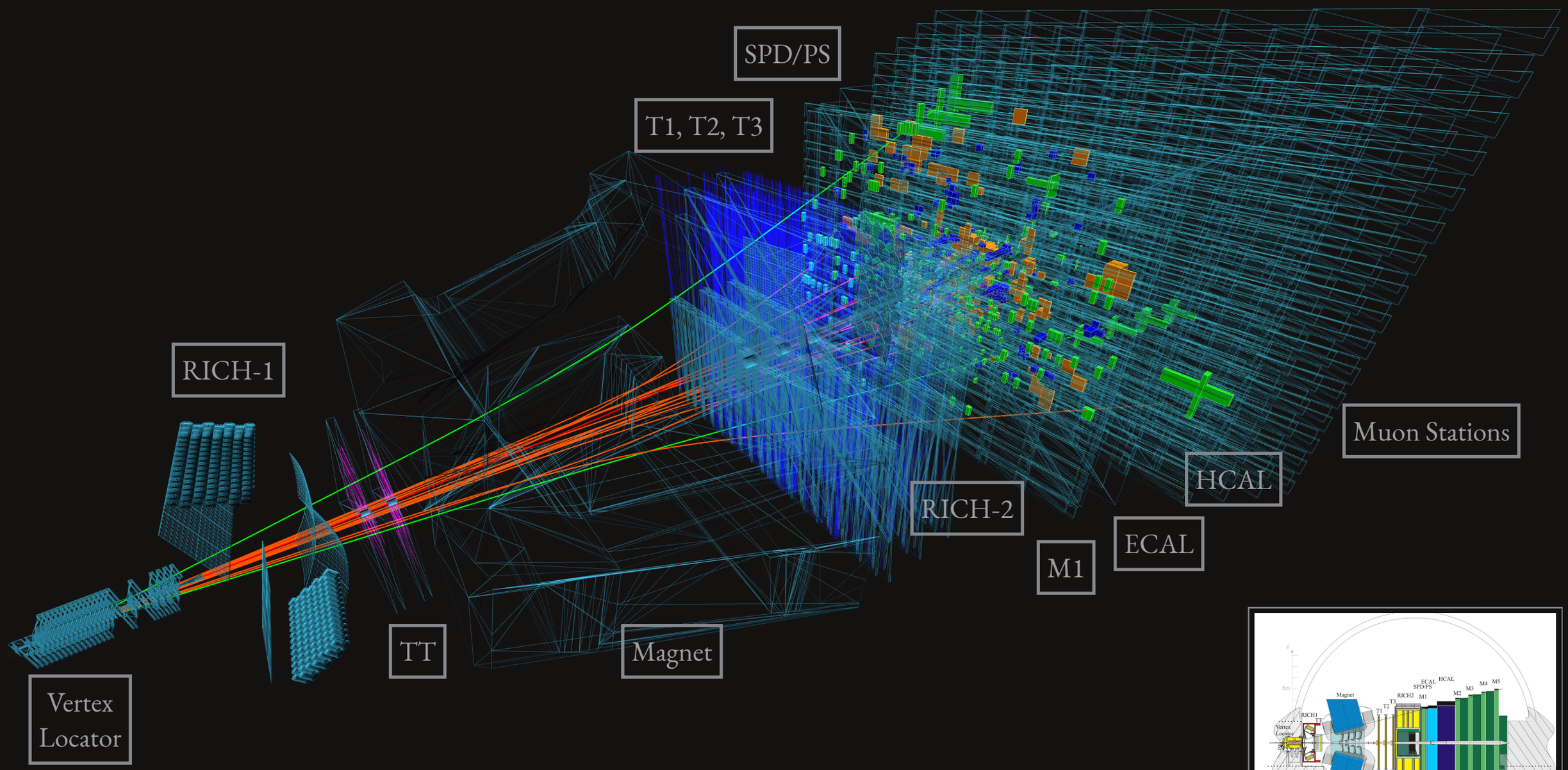

[Int. J. Mod. Phys. A30, (2015) 1530022]

[Backup]

CP-Averaged Angular Observables

S_i observables in the region between [1.1, 6.0] GeV

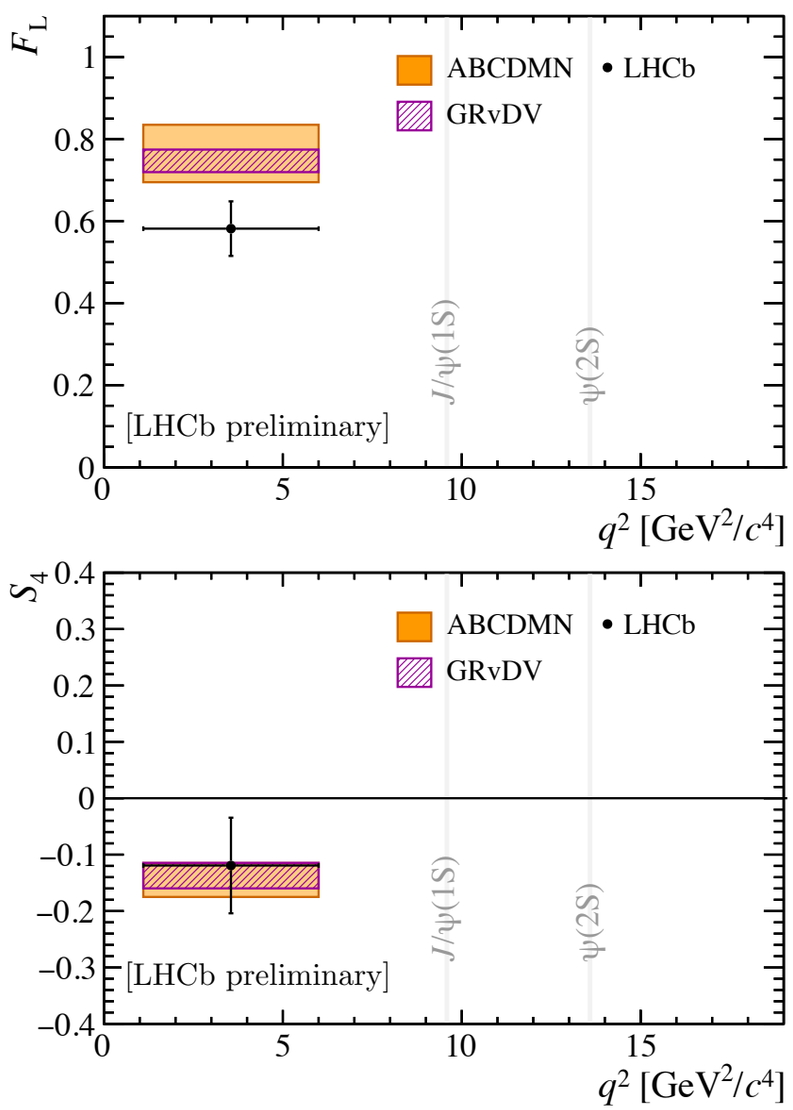

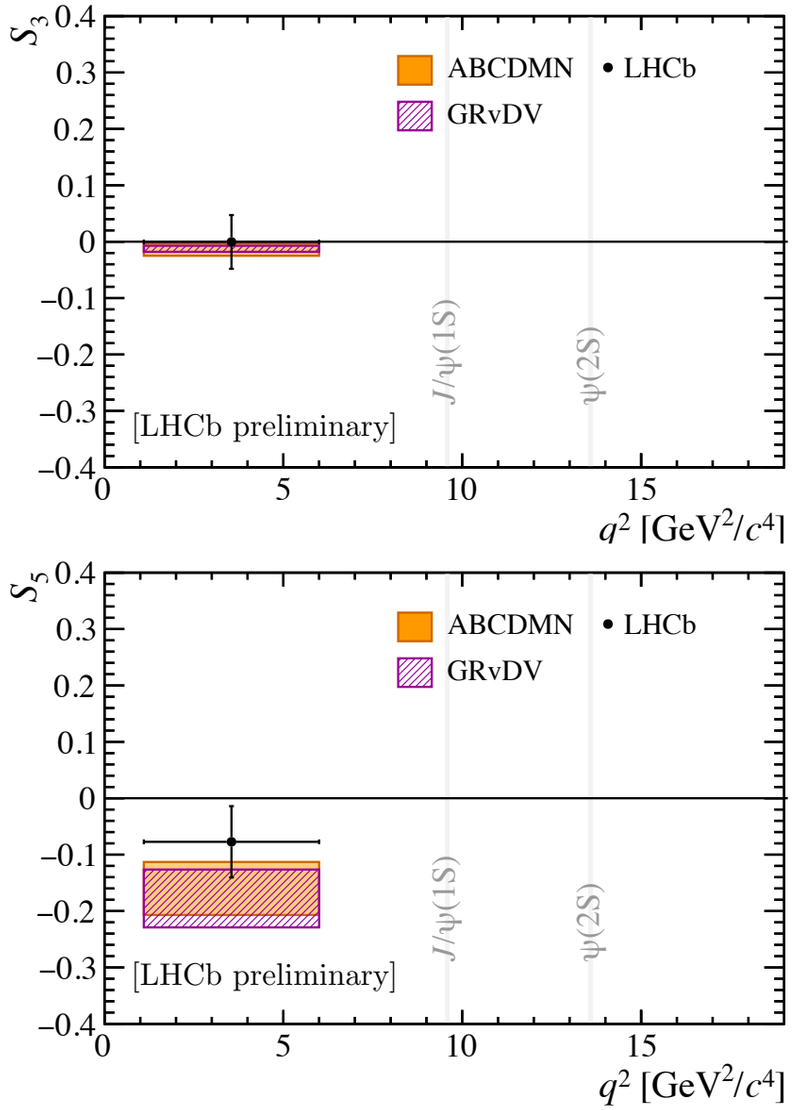

[N. Gubernari, M. Reboud, D. Van Dyk, J. Virto, JHEP 09 (2022) 133

[M. Algueró, A. Biswas, B.Capdevila, S. Descotes-Genon, J. Matias, EPJC 83 (2023) 7, 648

CP-Averaged Angular Observables

S_i observables in the region between [1.1, 6.0] GeV

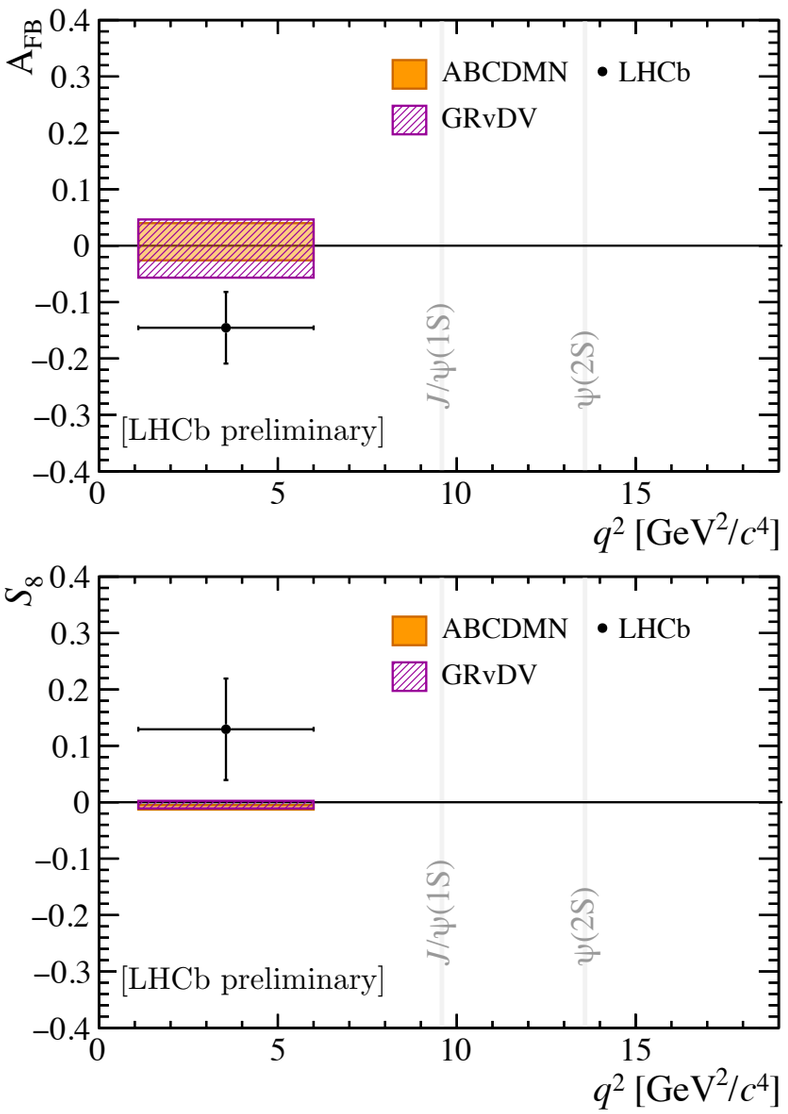

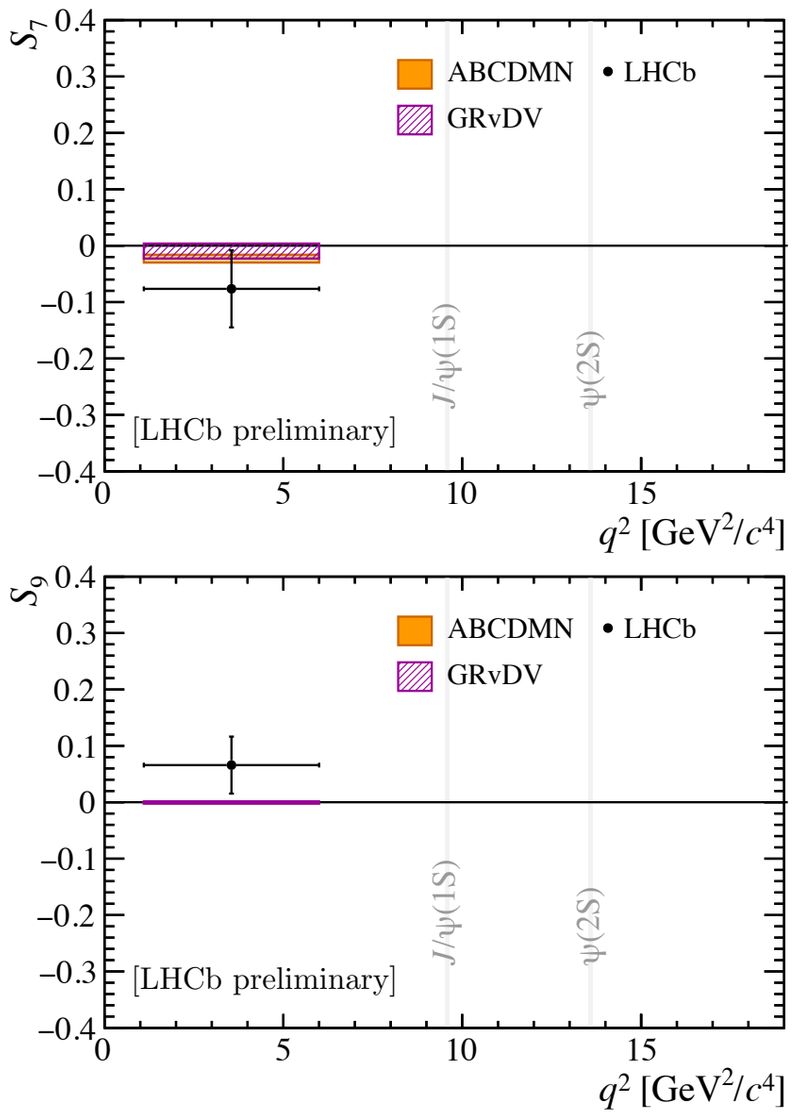

[N. Gubernari, M. Reboud, D. Van Dyk, J. Virto, JHEP 09 (2022) 133

[M. Algueró, A. Biswas, B.Capdevila, S. Descotes-Genon, J. Matias, EPJC 83 (2023) 7, 648

CP-Averaged Angular Observables

$P_i^{(\prime)}$ observables in the region between [1.1, 6.0] GeV

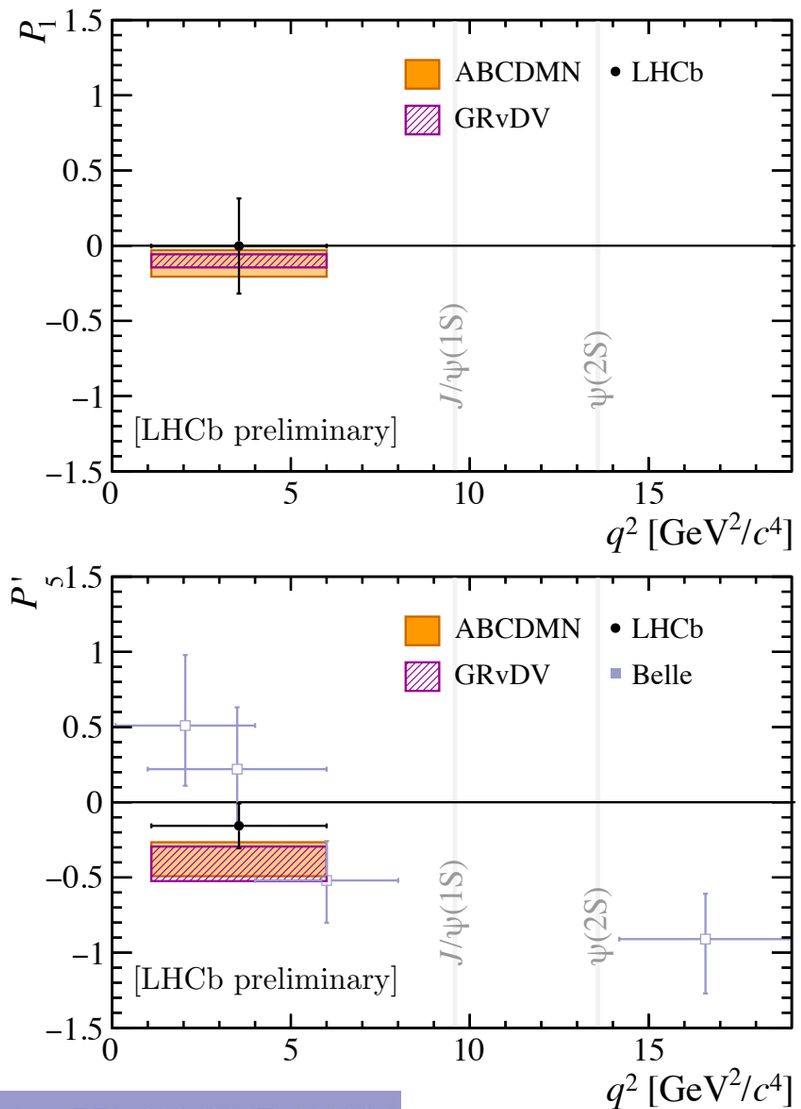

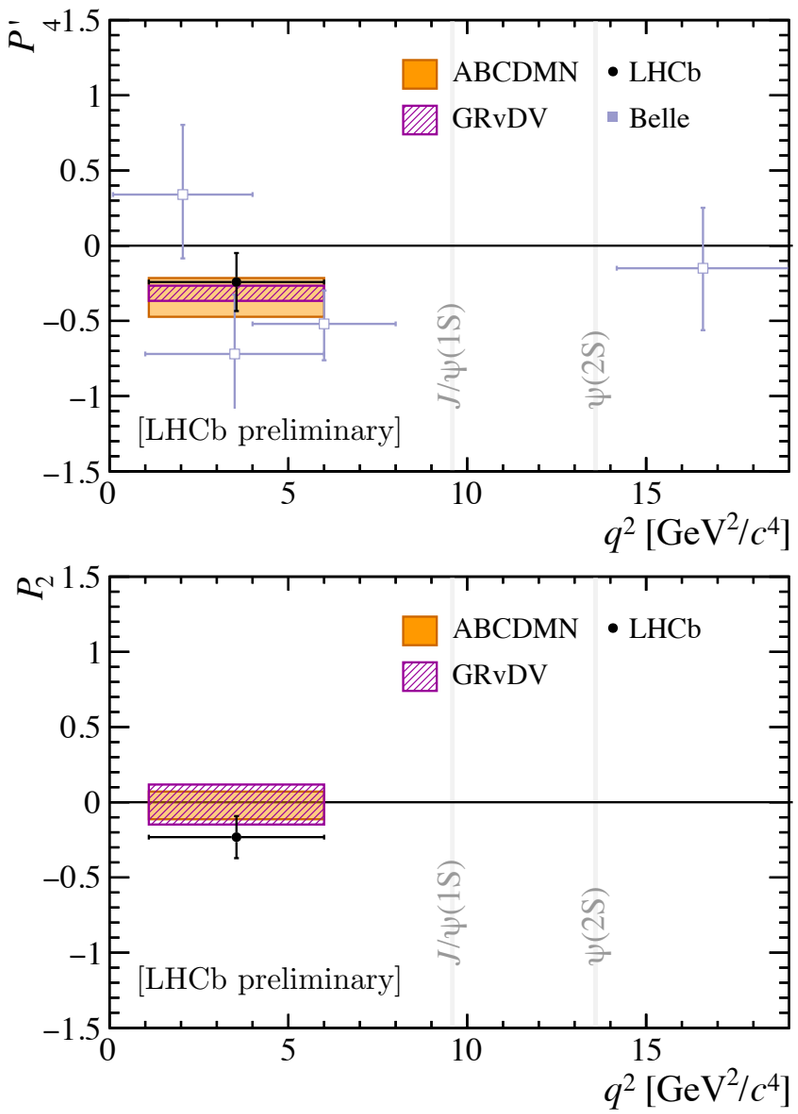

[Belle Collaboration, PRL 118 (2017) 111801

[N. Gubernari, M. Reboud, D. Van Dyk, J. Virto, JHEP 09 (2022) 133

[M. Algueró, A. Biswas, B.Capdevila, S. Descotes-Genon, J. Matias, EPJC 83 (2023) 7, 648

CP-Averaged Angular Observables

$P_i^{(\prime)}$ observables in the region between [1.1, 6.0] GeV

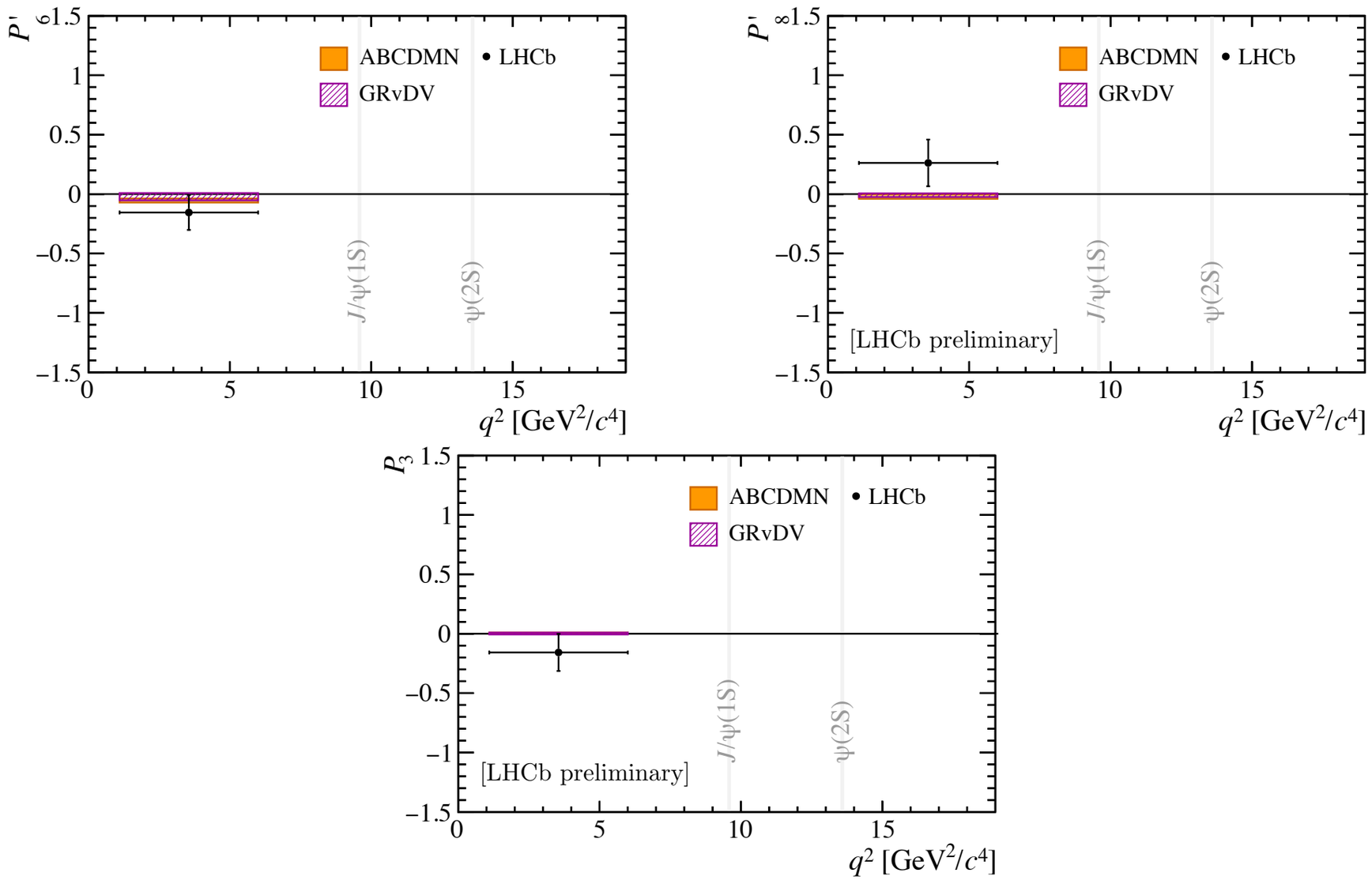

[N. Gubernari, M. Reboud, D. Van Dyk, J. Virto, JHEP 09 (2022) 133

[M. Algueró, A. Biswas, B.Capdevila, S. Descotes-Genon, J. Matias, EPJC 83 (2023) 7, 648

$S_i/P_i^{(\prime)}$ Correlation Matrix

S_i observables in the region between [1.1, 6.0] GeV

[Statistical]

	F_L	S_3	S_4	S_5	A_{FB}	S_7	S_8	S_9
F_L	1.00	0.01	−0.07	0.00	0.06	−0.01	−0.04	−0.06
S_3		1.00	−0.07	−0.02	0.05	0.10	−0.08	−0.01
S_4			1.00	−0.10	−0.10	−0.07	0.09	0.09
S_5				1.00	−0.05	0.06	−0.04	−0.03
A_{FB}					1.00	0.11	−0.07	−0.06
S_7						1.00	−0.07	−0.14
S_8							1.00	−0.01
S_9								1.00

[Systematics]

	F_L	S_3	S_4	S_5	A_{FB}	S_7	S_8	S_9
F_L	1.000	0.008	−0.105	−0.151	−0.226	−0.015	0.014	−0.051
S_3		1.000	0.004	−0.055	0.002	0.007	0.015	0.014
S_4			1.000	0.354	0.013	−0.038	0.001	0.006
S_5				1.000	0.084	0.000	−0.033	0.007
A_{FB}					1.000	−0.017	−0.006	0.014
S_7						1.000	0.089	−0.044
S_8							1.000	−0.004
S_9								1.000

$P_i^{(\prime)}$ observables in the region between [1.1, 6.0] GeV

[Statistical]

	F_L	P_1	P_2	P_3	P_4'	P_5'	P_6'	P_8'
F_L	1.00	0.02	−0.20	−0.08	−0.09	−0.02	−0.02	−0.01
P_1		1.00	0.04	0.01	−0.07	−0.02	0.10	−0.08
P_2			1.00	0.06	−0.07	−0.05	0.11	−0.06
P_3				1.00	−0.08	0.03	0.14	0.02
P_4'					1.00	−0.10	−0.07	0.09
P_5'						1.00	0.06	−0.03
P_6'							1.00	−0.07
P_8'								1.00

[Systematics]

	F_L	P_1	P_2	P_3	P_4'	P_5'	P_6'	P_8'
F_L	1.00	−0.041	−0.142	0.023	−0.223	−0.326	−0.025	0.011
P_1		1.000	0.009	−0.012	0.001	−0.030	−0.009	0.009
P_2			1.000	0.017	0.067	0.127	0.016	−0.001
P_3				1.000	−0.004	0.002	0.042	0.004
P_4'					1.000	0.418	−0.010	0.000
P_5'						1.000	0.018	−0.025
P_6'							1.000	0.089
P_8'								1.000

CP-Averaged Angular Observables

	$1.1 < q^2 < 7.0\,\mathrm{GeV}^2/\mathrm{c}^4$		
F_L	$0.581 \pm 0.041 \pm 0.049$		
S_3	$-0.011 \pm 0.039 \pm 0.023$	P_1	$-0.053 \pm 0.188 \pm 0.199$
S_4	$-0.119 \pm 0.063 \pm 0.041$	P_4'	$-0.242 \pm 0.128 \pm 0.109$
S_5	$-0.096 \pm 0.049 \pm 0.035$	P_5'	$-0.194 \pm 0.100 \pm 0.097$
A_FB	$-0.140 \pm 0.046 \pm 0.036$	P_2	$-0.223 \pm 0.074 \pm 0.090$
S_7	$-0.062 \pm 0.052 \pm 0.038$	P_6'	$-0.125 \pm 0.106 \pm 0.088$
S_8	$0.061 \pm 0.065 \pm 0.042$	P_8'	$0.123 \pm 0.131 \pm 0.098$
S_9	$0.069 \pm 0.042 \pm 0.019$	P_3	$-0.165 \pm 0.100 \pm 0.084$

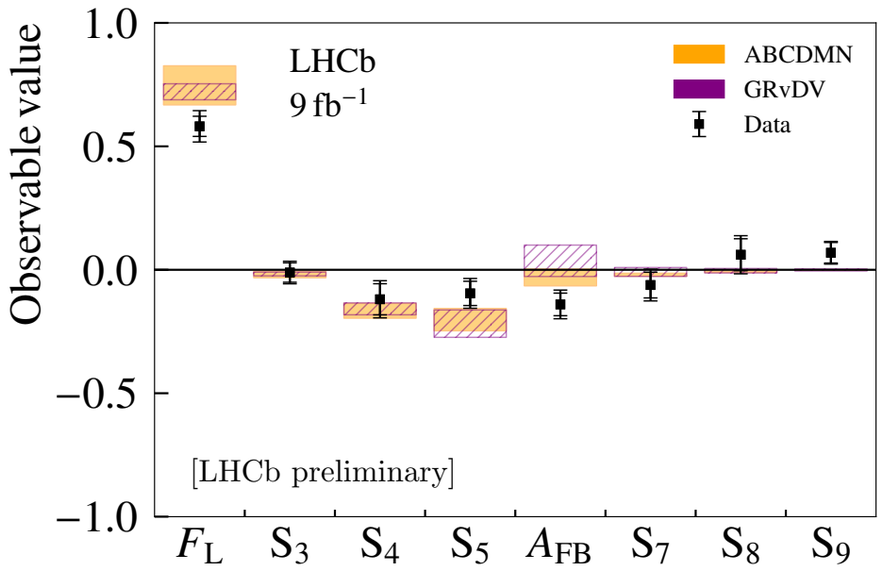

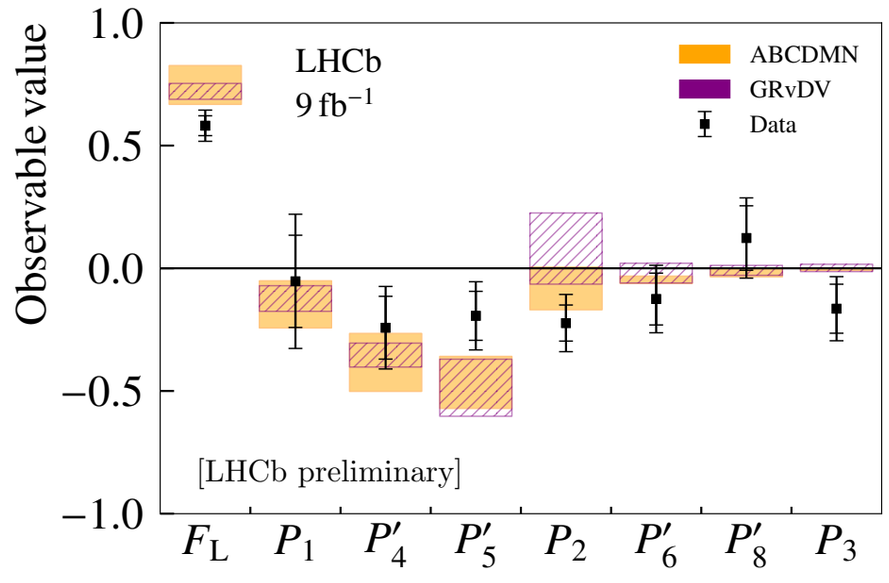

[N. Gubernari, M. Reboud, D. Van Dyk, J. Virto, JHEP 09 (2022) 133

[M. Algueró, A. Biswas, B.Capdevila, S. Descotes-Genon, J. Matias, EPJC 83 (2023) 7, 648

$S_i/P_i^{(\prime)}$ Correlation Matrix

S_i observables in the region between [1.1, 7.0] GeV

[Statistical]

	F_L	S_3	S_4	S_5	A_{FB}	S_7	S_8	S_9
F_L	1.0	0.02	−0.05	−0.01	0.09	−0.05	−0.03	−0.05
S_3		1.00	−0.05	−0.03	0.04	0.05	−0.05	0.02
S_4			1.00	−0.10	−0.14	−0.05	0.06	0.04
S_5				1.00	−0.07	0.06	−0.02	−0.04
A_{FB}					1.00	0.03	−0.04	−0.01
S_7						1.00	−0.06	−0.13
S_8							1.00	−0.04
S_9								1.00

[Systematics]

	F_L	S_3	S_4	S_5	A_{FB}	S_7	S_8	S_9
F_L	1.000	0.010	−0.089	−0.134	−0.170	−0.016	0.015	−0.043
S_3		1.000	0.003	−0.049	−0.002	0.004	0.017	0.010
S_4			1.000	0.328	−0.008	−0.038	0.004	0.002
S_5				1.000	0.053	0.003	−0.04	−0.002
A_{FB}					1.000	−0.021	−0.006	0.011
S_7						1.000	0.114	−0.050
S_8							1.000	−0.006
S_9								1.000

$P_i^{(\prime)}$ observables in the region between [1.1, 7.0] GeV

[Statistical]

	F_L	P_1	P_2	P_3	P_4'	P_5'	P_6'	P_8'
F_L	1.00	0.00	−0.18	−0.11	−0.07	−0.04	−0.06	−0.02
P_1		1.00	0.04	−0.02	−0.05	−0.03	0.05	−0.05
P_2			1.00	0.03	−0.13	−0.06	0.05	−0.03
P_3				1.00	−0.03	0.04	0.14	0.04
P_4'					1.00	−0.10	−0.05	0.06
P_5'						1.00	0.06	−0.02
P_6'							1.00	−0.06
P_8'								1.00

[Systematics]

	F_L	P_1	P_2	P_3	P_4'	P_5'	P_6'	P_8'
F_L	1.00	−0.037	−0.052	0.021	−0.185	−0.276	−0.023	0.009
P_1		1.00	0.004	−0.022	0.018	−0.014	0.005	0.016
P_2			1.00	0.009	−0.011	0.031	−0.008	0.000
P_3				1.000	−0.006	0.009	0.053	0.009
P_4'					1.000	0.368	−0.026	0.004
P_5'						1.000	0.011	−0.030
P_6'							1.000	0.113
P_8'								1.000

LFU Observables

	$1.1 < q^2 < 6.0\,\mathrm{GeV}^2/c^4$
Q_{F_L}	$0.121 \pm 0.050 \pm 0.050$
Q_1	$-0.097 \pm 0.264 \pm 0.246$
Q_4	$-0.071 \pm 0.173 \pm 0.120$
Q_5	$0.045 \pm 0.132 \pm 0.102$
Q_2	$0.066 \pm 0.098 \pm 0.112$
Q_6	$-0.049 \pm 0.137 \pm 0.092$
Q_8	$-0.275 \pm 0.166 \pm 0.137$
Q_3	$0.216 \pm 0.144 \pm 0.110$

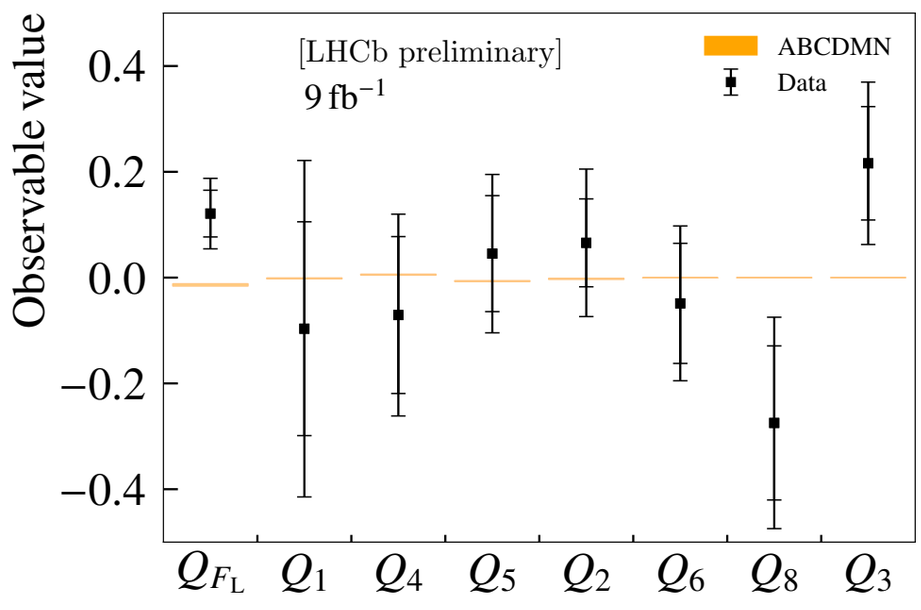

	$1.1 < q^2 < 7.0\,\mathrm{GeV}^2/\mathrm{c}^4$
Q_{F_L}	$0.126 \pm 0.046 \pm 0.049$
Q_1	$-0.034 \pm 0.246 \pm 0.199$
Q_4	$-0.131 \pm 0.149 \pm 0.109$
Q_5	$-0.014 \pm 0.119 \pm 0.097$
Q_2	$0.109 \pm 0.086 \pm 0.091$
Q_6	$-0.080 \pm 0.124 \pm 0.088$
Q_8	$-0.152 \pm 0.149 \pm 0.098$
Q_3	$0.205 \pm 0.131 \pm 0.084$

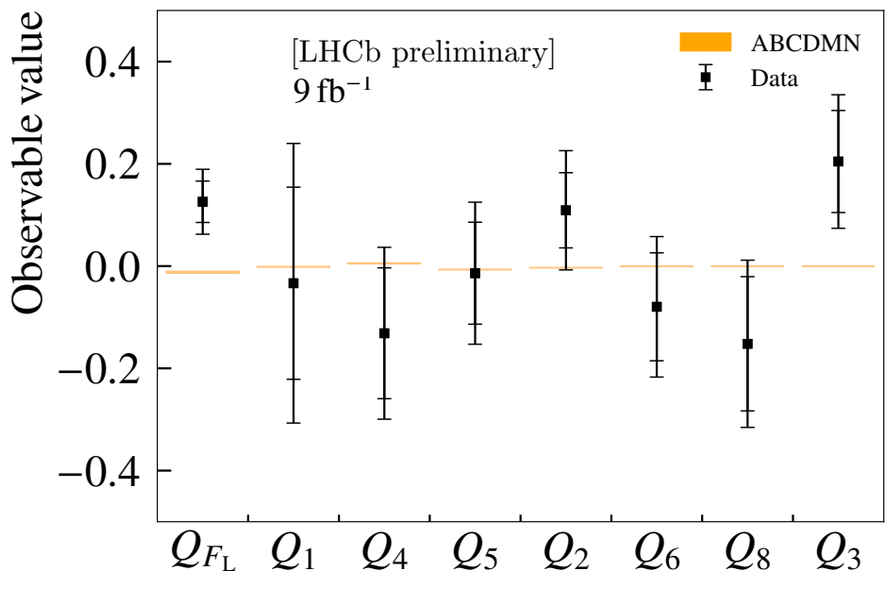

[M. Algueró, A. Biswas, B.Capdevila, S. Descotes-Genon, J. Matias, EPJC 83 (2023) 7, 648

LFU Observables

	$1.1 < q^2 < 6.0\,\mathrm{GeV}^2/c^4$
Q_{F_L}	$0.121 \pm 0.050 \pm 0.050$
Q_1	$-0.097 \pm 0.264 \pm 0.246$
Q_4	$-0.071 \pm 0.173 \pm 0.120$
Q_5	$0.045 \pm 0.132 \pm 0.102$
Q_2	$0.066 \pm 0.098 \pm 0.112$
Q_6	$-0.049 \pm 0.137 \pm 0.092$
Q_8	$-0.275 \pm 0.166 \pm 0.137$
Q_3	$0.216 \pm 0.144 \pm 0.110$

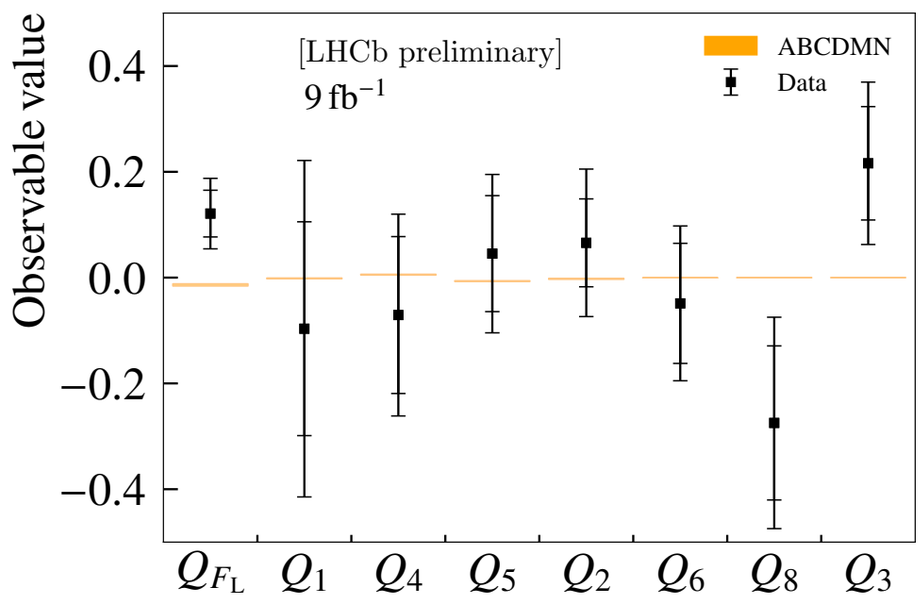

	$1.1 < q^2 < 7.0\,\mathrm{GeV}^2/\mathrm{c}^4$
Q_{F_L}	$0.126 \pm 0.046 \pm 0.049$
Q_1	$-0.034 \pm 0.246 \pm 0.199$
Q_4	$-0.131 \pm 0.149 \pm 0.109$
Q_5	$-0.014 \pm 0.119 \pm 0.097$
Q_2	$0.109 \pm 0.086 \pm 0.091$
Q_6	$-0.080 \pm 0.124 \pm 0.088$
Q_8	$-0.152 \pm 0.149 \pm 0.098$
Q_3	$0.205 \pm 0.131 \pm 0.084$

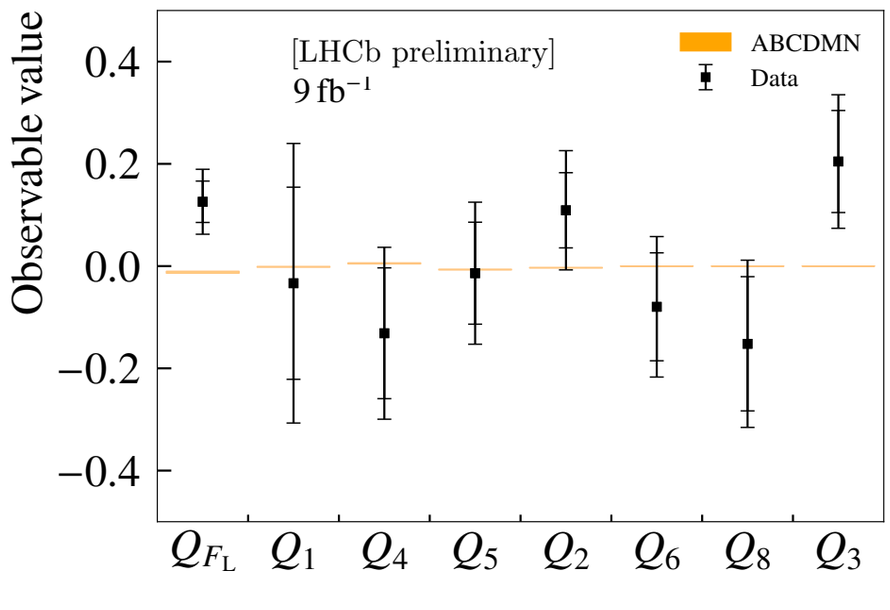

[M. Algueró, A. Biswas, B.Capdevila, S. Descotes-Genon, J. Matias, EPJC 83 (2023) 7, 648

[Backup]

MISIDENTIFIED BACKGROUND PROCEDURE

[PRL 131 (2023) 051803, PRD 108 (2023) 032002]

TIGHTENING ELECTRON PID EXHIBITS A COHERENT PATTERN

INVERT PID REQUIREMENTS ON ONE OR BOTH ELECTRONS (CONTROL CHANNEL)

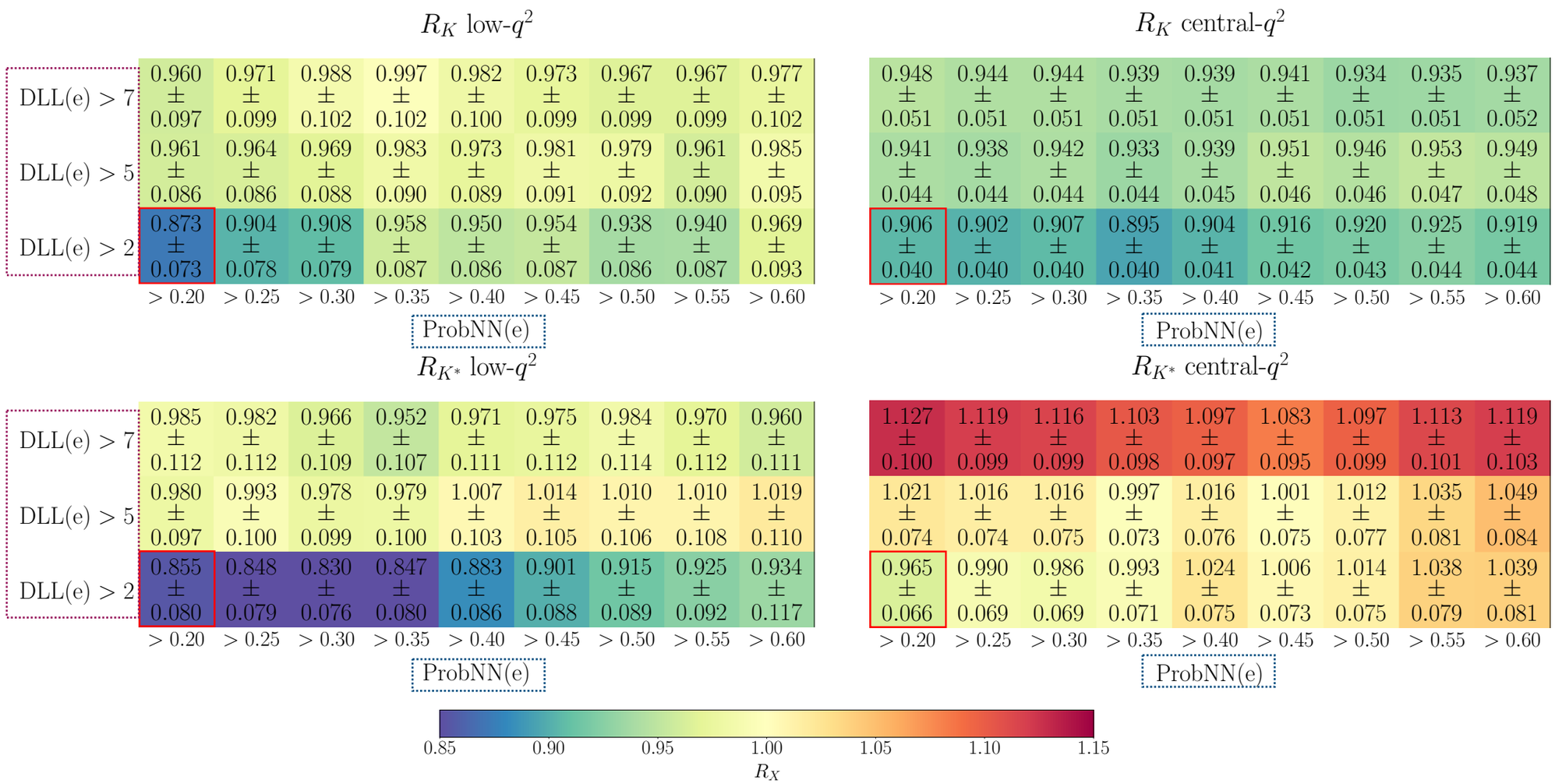

DLL(E): COMBINATION OF SUB-DETECTORS DELTA LOG-LIKEHOOD FOR π, e

PROBNN(E): NEURAL-NET BASED E-ID SCORE

[Backup]

Misidentified background procedure

Example from [PRL 131 (2023) 051803, PRD 108 (2023) 032002]

Invert PID Requirements on One or Both Electrons (Control Channel)

Control Regions

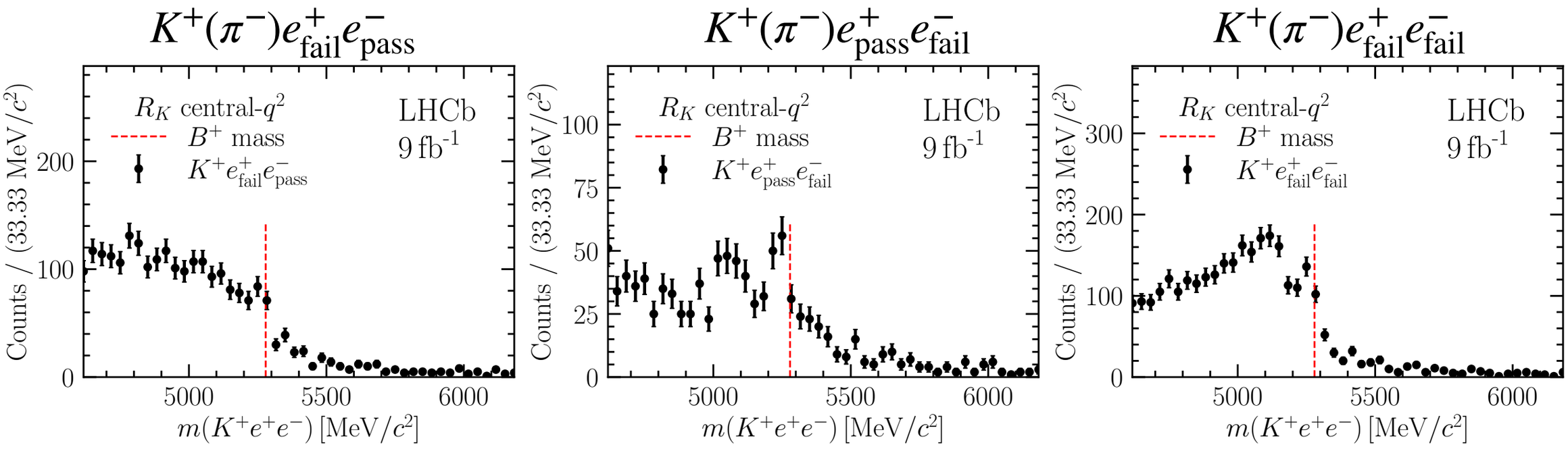

Categorise Pion- and Kaon-like Electrons in Control Region with Neural-net ID

Parametrise Shape and Predict Normalisation of Such Contribution

MISIDENTIFIED BACKGROUND PROCEDURE

EXAMPLE FROM [PRL 131 (2023) 051803, PRD 108 (2023) 032002]

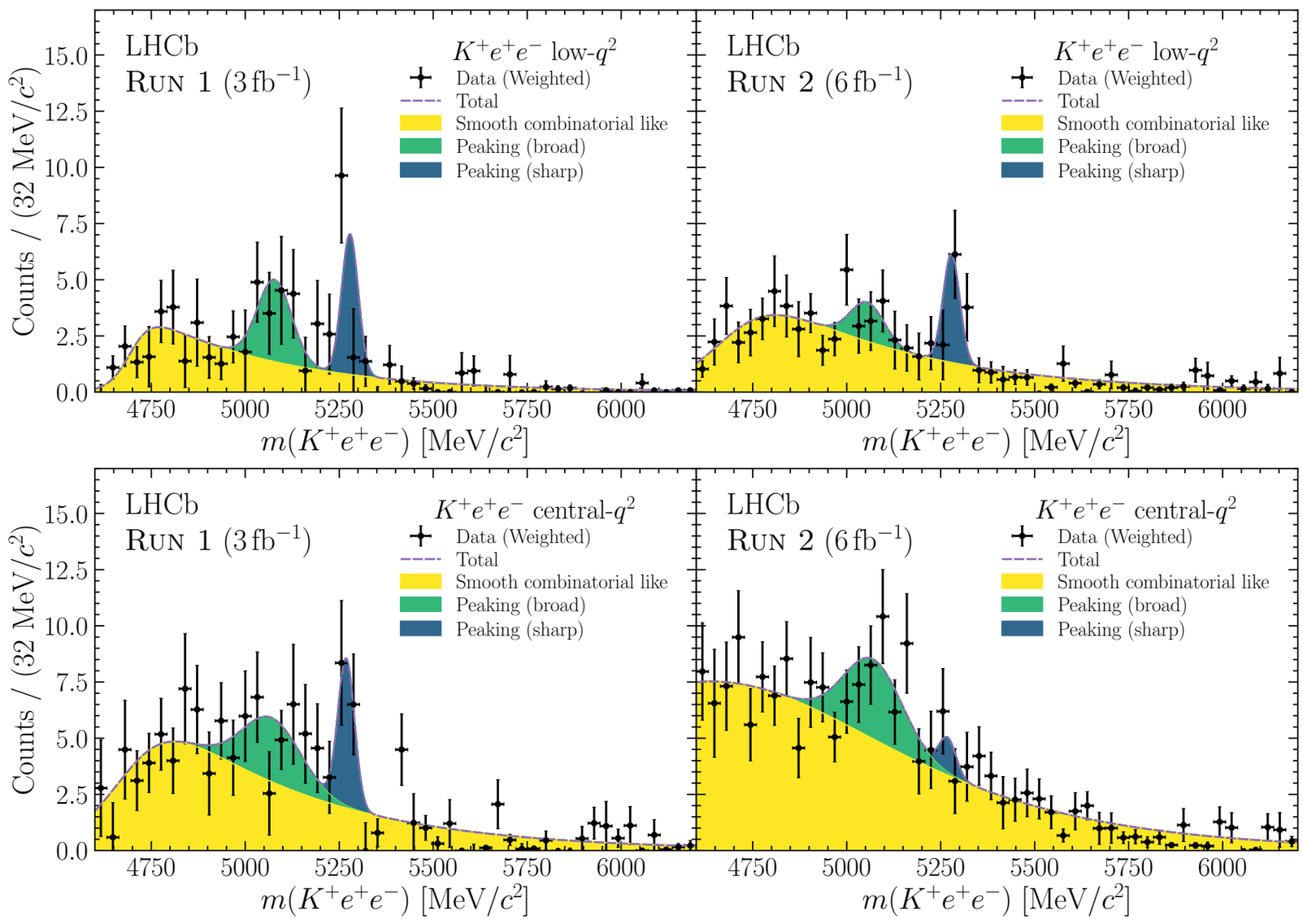

SIMILAR MISIDENTIFIED BACKGROUND MODELLING FOR R_{K^*}

MISIDENTIFIED BACKGROUND PROCEDURE

EXAMPLE FROM [PRL 131 (2023) 051803, PRD 108 (2023) 032002]